AGU ADVANCING EARTH AND SPACE SCIENCES

Water Resources Research

RESEARCH ARTICLE
10.1029/2023WR035928

Seasonal and Species-Level Water-Use Strategies and Groundwater Dependence in Dryland Riparian Woodlands During Extreme Drought

Jared Williams[1,2], John C. Stella[3], Michael Bliss Singer[4,5,6], Adam M. Lambert[2,7], Steven L. Voelker[8], John E. Drake[3], Jonathan M. Friedman[9], Lissa Pelletier[1], Li Kui[2,4], and Dar A. Roberts[4,10]

[1]Graduate Program in Environmental Science, College of Environmental Science and Forestry, State University of New York, Syracuse, NY, USA, [2]Marine Science Institute, University of California, Santa Barbara, Santa Barbara, CA, USA, [3]Department of Sustainable Resources Management, State University of New York College of Environmental Science and Forestry, Syracuse, NY, Unites States of America, [4]Earth Research Institute, University of California, Santa Barbara, Santa Barbara, CA, USA, [5]School of Earth and Environmental Sciences, Cardiff University, Cardiff, UK, [6]Water Research Institute, Cardiff University, Cardiff, UK, [7]Cheadle Center for Biodiversity and Ecological Restoration, University of California, Santa Barbara, Santa Barbara, CA, USA, [8]College of Forest Resources and Environmental Science, Michigan Technological University, Houghton, MI, USA, [9]U.S. Geological Survey, Fort Collins Science Center, Fort Collins, CO, USA, [10]Department of Geography, University of California, Santa Barbara, Santa Barbara, CA, USA

Abstract Drought-induced groundwater decline and warming associated with climate change are primary threats to dryland riparian woodlands. We used the extreme 2012–2019 drought in southern California as a natural experiment to assess how differences in water-use strategies and groundwater dependence may influence the drought susceptibility of dryland riparian tree species with overlapping distributions. We analyzed tree-ring stable carbon and oxygen isotopes collected from two cottonwood species (*Populus trichocarpa* and *P. fremontii*) along the semi-arid Santa Clara River. We also modeled tree source water $\delta^{18}O$ composition to compare with observed source water $\delta^{18}O$ within the floodplain to infer patterns of groundwater reliance. Our results suggest that both species functioned as facultative phreatophytes that used shallow soil moisture when available but ultimately relied on groundwater to maintain physiological function during drought. We also observed apparent species differences in water-use strategies and groundwater dependence related to their regional distributions. *P. fremontii* was constrained to more arid river segments and ostensibly used a greater proportion of groundwater to satisfy higher evaporative demand. *P. fremontii* maintained $\Delta^{13}C$ at pre-drought levels up until the peak of the drought, when trees experienced a precipitous decline in $\Delta^{13}C$. This response pattern suggests that trees prioritized maintaining photosynthetic processes over hydraulic safety, until a critical point. In contrast, *P. trichocarpa* showed a more gradual and sustained reduction in $\Delta^{13}C$, indicating that drought conditions induced stomatal closure and higher water use efficiency. This strategy may confer drought avoidance for *P. trichocarpa* while increasing its susceptibility to anticipated climate warming.

Key Points:

- Dryland riparian cottonwoods used shallow soil moisture when available but ultimately relied on groundwater for survival during drought
- Species had different water-use strategies related to their distribution along a gradient of increasing aridity with distance from coast
- *Populus trichocarpa* appears more susceptible to warming, and *P. fremontii* more vulnerable to groundwater decline due to high water demand

Supporting Information:

Supporting Information may be found in the online version of this article.

Correspondence to:

J. Williams,
jaredwilliams@ucsb.edu

Citation:

Williams, J., Stella, J. C., Singer, M. B., Lambert, A. M., Voelker, S. L., Drake, J. E., et al. (2024). Seasonal and species-level water-use strategies and groundwater dependence in dryland riparian woodlands during extreme drought. *Water Resources Research*, *60*, e2023WR035928. https://doi.org/10.1029/2023WR035928

Received 24 JULY 2023
Accepted 22 MAR 2024

Author Contributions:

Conceptualization: Jared Williams, John C. Stella, Steven L. Voelker, John E. Drake, Jonathan M. Friedman
Data curation: Jared Williams, Li Kui
Formal analysis: Jared Williams, Michael Bliss Singer
Funding acquisition: Jared Williams, John C. Stella, Michael Bliss Singer, Adam M. Lambert, Dar A. Roberts
Investigation: Jared Williams, Lissa Pelletier, Li Kui

1. Introduction

Riparian woodlands are productive and biodiverse ecosystems in dryland regions that owe their persistence in the landscape to groundwater (Bateman & Merritt, 2020; Sabathier et al., 2021; Singer et al., 2014; Stella et al., 2013). Most dryland riparian trees are assumed to be phreatophytes that rely on consistent root access to groundwater to tolerate seasonally intermittent precipitation and high vapor pressure deficits (Hultine et al., 2020); as such, they are highly susceptible to groundwater decline (Rood et al., 2003; Stromberg et al., 1996). In dryland regions, climate change is expected to increase the frequency and severity of drought events, accompanied by warmer temperatures (Li et al., 2021), contributing to more severe drought-induced groundwater decline (Dragoni & Sukhija, 2008). The effects of these hydroclimatic stressors are exacerbated by human land conversion and groundwater extraction, which collectively threaten the persistence of these ecosystems in their current state and distribution (Krueper, 1993; NRC, 2002; Stella & Bendix, 2019).

The population decline of cottonwoods and poplars (*Populus* spp.) is of particular concern, as these are foundation species in dryland riparian communities, and interacting stressors have diminished their range and abundance throughout western North America over recent decades (Braatne et al., 2007; Howe & Knopf, 1991; Lite & Stromberg, 2005). Groundwater decline in particular is a well-documented threat to their persistence (Kibler

Methodology: Jared Williams, Lissa Pelletier
Project administration: Jared Williams, John C. Stella
Resources: Adam M. Lambert
Supervision: John C. Stella, Adam M. Lambert, Steven L. Voelker
Visualization: Jared Williams, John C. Stella
Writing – original draft: Jared Williams, John C. Stella, Adam M. Lambert
Writing – review & editing: Michael Bliss Singer, Steven L. Voelker, John E. Drake, Jonathan M. Friedman, Dar A. Roberts

et al., 2021; Rood et al., 2003; Scott et al., 1999; Williams et al., 2022). Cottonwoods have been described as both obligate (Andersen, 2016; Busch et al., 1992; Rood et al., 2013) and facultative phreatophytes (Hultine et al., 2010; Rood et al., 2011; Stromberg et al., 1996), depending on the species and the specific hydroclimatic regimes in which they were established (Hultine et al., 2020). Species that inhabit more arid regions have prodigious water requirements to meet greater atmospheric demand, which intensifies their dependence on groundwater (Hultine et al., 2020; Voltas et al., 2015). Consequently, increasing evaporative demand associated with climate change represents a compound stressor for cottonwoods and other phreatophytes that increases their susceptibility to drought and associated groundwater decline (Williams et al., 2022).

Stomatal closure is the most immediate drought-coping mechanism for plants to regulate transpirational water loss, which helps maintain stem water potential above a critical threshold and prevent xylem embolism that can cumulatively induce hydraulic failure (Farooq et al., 2012; Martin-StPaul et al., 2017; Pirasteh-Anosheh et al., 2016). At the same time, stomatal closure leads to higher internal leaf temperatures and consequently increases the risk of heat stress when drought is accompanied by high temperatures (Blasini et al., 2022). However, groundwater provides a perennial water source that can buffer dryland riparian trees from the effects of atmospheric drought and rising temperatures (Wang et al., 2023). Therefore, consistent access to groundwater may represent the only feasible means of persistence for riparian trees in regions where droughts and warming are becoming more extreme with climate change.

The effects of climate change may differentially affect dryland riparian tree species based on their water-use strategies, drought susceptibility, and the extent of their groundwater dependence. In this context, carbon and oxygen stable isotopes in tree rings can be used to investigate historical patterns of drought response and source water use to infer future responses of dryland riparian woodlands to climate change and groundwater decline. Carbon isotope discrimination ($\Delta^{13}C$) derived from tree rings provides a retrospective measure of canopy-integrated leaf gas-exchange (Cernusak et al., 2013; Farquhar et al., 1989; Francey & Farquhar, 1982), making it a useful tool to evaluate past drought responses of plants (Klein et al., 2013). Within the same tree-ring series, stable oxygen isotope ratios ($\delta^{18}O$) can be used to infer changes in source water use (Ehleringer & Dawson, 1992; Sargeant et al., 2019) and utilized in coordination with $\Delta^{13}C$ to investigate plant ecohydrologic responses (Altieri et al., 2015; Battipaglia & Cherubini, 2022; Gessler et al., 2018; Moreno-Gutiérrez et al., 2012).

The environmental processes that determine $\Delta^{13}C$ and $\delta^{18}O$ composition in tree-rings derive from different fractionation mechanisms. $\Delta^{13}C$ reflects the ratio of leaf internal CO^2 concentration to atmospheric CO^2 concentration (C_i/C_a), and the $\Delta^{13}C$ signal in tree rings is therefore determined by the balance between the rate of assimilation (i.e., photosynthesis) and leaf gas-exchange (i.e., stomatal conductance) over the growing season, where an increase in photosynthesis or a decrease in stomatal conductance results in lower values of $\Delta^{13}C$, and vice versa. For vegetation in dryland systems that are not light-limited, stomatal conductance is the dominant influence on C_i/C_a, and decreases in $\Delta^{13}C$ are often attributed to stomatal closure in response to drought stress (McCarroll & Loader, 2004).

For $\delta^{18}O$, the leaf water pool signal that is imprinted in tree-ring cellulose reflects to a great extent the isotopic signal of source water, which does not fractionate during root water uptake; therefore, variation in $\delta^{18}O$ values over time can indicate a relative shift in tree water sources (Dawson & Ehleringer, 1998). Water in the vadose zone (shallower soil layers) is subject to evaporative loss making it isotopically enriched relative to groundwater (Dawson & Ehleringer, 1998; Singer et al., 2013). This pattern allows for differentiation among plant water sources at different depths along the soil profile and can be useful for evaluating tree dependence on groundwater, which is typically depleted in $\delta^{18}O$, versus shallow moisture sources (Sargeant & Singer, 2016). In addition, $\delta^{18}O$ in plant tissues reflects changes in vapor pressure deficit because evaporative demand causes enrichment of leaf water that is also recorded in tree-ring cellulose (Barbour, 2007). Consequently, enriched (higher) values of $\delta^{18}O$ are often associated with stomatal closure in response to greater evaporative demand (Barbour & Farquhar, 2000; Scheidegger et al., 2000), yet this signal can be overpowered when changes in source water are considerable (Barbour et al., 2004; Sarris et al., 2013; Treydte et al., 2014). Additional influences on tree-ring $\delta^{18}O$ include diffusion of water vapor from the air into leaves during humid conditions, mixing of leaf water with unenriched stem water (the Péclet effect), and post-photosynthetic processes that may complicate interpretations of leaf-level processes (Barbour, 2007; Gessler et al., 2014; Roden et al., 2000). Recently developed mechanistic models can account for many of these influences and allow for the estimation of source water $\delta^{18}O$ based on tree-ring $\delta^{18}O$,

facilitating direct comparisons with endmember $\delta^{18}O$ composition to better infer plant water sources (Sargeant et al., 2019).

In this study, we used isotope dendrochronologies to build upon Williams et al. (2022)'s investigation of riparian cottonwood (*Populus trichocarpa* and *P. fremontii*) responses to the extreme 2012–2019 drought, along the largest free-flowing river in southern California. Previously, we found that $\Delta^{13}C$ and annual growth of cottonwoods along the semi-arid Santa Clara River exhibited a coordinated drought response, determined by the severity of multi-year groundwater decline, and that trees subjected to faster rates of groundwater decline showed greater stomatal sensitivity to increasing atmospheric demand. Here, we incorporate semi-annual $\delta^{18}O$ data from the same trees and time period to evaluate seasonal changes and species differences in water-use strategies during the drought. Our goals were to determine (a) how riparian tree water sources and water-use strategies changed seasonally and interannually in response to drought conditions, and (b) whether water-use strategies and drought susceptibility differed between cottonwood species with overlapping distributions. Whereas the previous study used tree-ring $\Delta^{13}C$ and annual growth to evaluate drivers and indicators of drought stress shared among dryland riparian phreatophytes, the present study employs a dual isotope ($\Delta^{13}C$ and $\delta^{18}O$) approach to investigate the extent to which riparian cottonwood species are obligate versus facultative phreatophytes and to infer potential differences in climate change vulnerability for species with differing water-use strategies.

2. Materials and Methods

2.1. Site and Species Description

The Santa Clara River drains a watershed of 4,204 km^2 in southern California (Figure 1) and produces an average annual water yield greater than 0.124 km^3 (Birosik, 2006; Brownlie & Taylor, 1981). Mean annual precipitation varies from 35 cm where the river meets the Pacific Ocean to <20 cm at the easternmost extent of the catchment (Beller et al., 2016; Downs et al., 2013). Precipitation is generally confined to the rainy season (October - March) and conditions become increasingly arid over the course of the growing season. Groundwater recharge occurs at the highest rates during episodic flooding events in the winter (Andrews et al., 2004; Cayan et al., 1999), and the water table can decline markedly during extended periods of low rainfall (Kibler et al., 2021).

The Santa Clara River is an intermittent river composed of gaining (wetter) and losing (dryer) reaches, which largely determine vegetation composition (Beller et al., 2016). Wetter reaches are composed of dense willow-cottonwood forests that host a significant proportion of regional biodiversity (Bennett et al., 2022; Hall et al., 2020). Two cottonwood species are foundational components of riparian forests in the catchment and region, with their distributions related to a gradient of increasing aridity with distance from the coast (Orr et al., 2011; Figure 1). Black cottonwood (*P. trichocarpa*, Torr. & A. Gray) is abundant where the coastal influence is strong but is largely absent in more arid upstream reaches. Fremont cottonwood (*P. fremontii*, S. Watson) is increasingly abundant with distance from the coast and becomes the dominant tree species in the warmer, interior portion of the catchment. This pattern matches the distributions of these species throughout North America, with *P. trichocarpa* found in wetter and more temperate regions and *P. fremontii* in more arid landscapes (Braatne et al., 1996; Cooke & Rood, 2007).

The meteorological drought in southern California that extended from 2012 to 2019 was the most extreme on record (Robeson, 2015; Warter et al., 2021). It was exacerbated by consecutive years of high temperature anomalies (Figure S1 in Supporting Information S1; Luo et al., 2017; Mann & Gleick, 2015), which combined with the drought caused severe soil moisture and groundwater depletion (Warter et al., 2021). These stressors triggered extensive mortality within riparian woodlands of the Santa Clara River during the peak of the drought (2013–2016) (Kibler et al., 2021), when drought conditions within the study area were classified from severe to exceptional (U.S. Drought Monitor, 2021), followed by a gradual recovery up until 2019.

2.2. Data Collection

Increment cores were collected in the summer of 2019 from 114 cottonwood trees (*P. trichocarpa* and *P. fremontii*) at seven sites along a 50-km stretch of the lower Santa Clara River (Figure 1; Table 1; Williams et al., 2022). The sampling sites spanned from Ventura County to Los Angeles County (river kilometers 18–71), including the transition zone where the marine influence on atmospheric conditions (i.e., fog) dissipates (Figure 1).

10.1029/2023WR035928

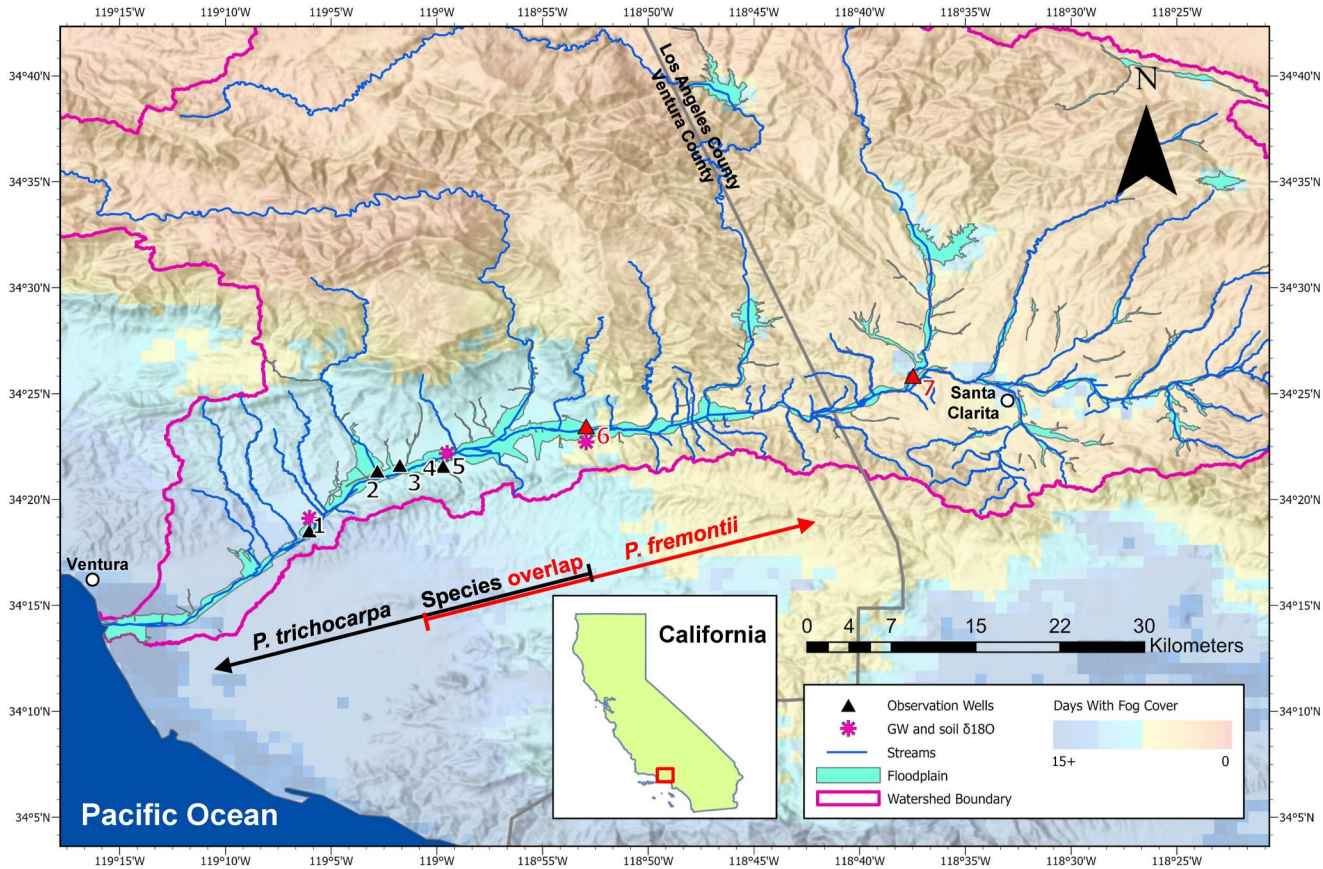

Figure 1. Site locations within the lower Santa Clara River, California. Sites containing *Populus trichocarpa* labeled in black: 1. Hanson, 2. South Mountain Road, 3. Hedrick Ranch Lower, 4. Hedrick Ranch Upper, and 5. Taylor. Sites containing *P. fremontii* labeled in red: 6. Fillmore Cienega and 7. Newhall Ranch. Groundwater observation wells associated with *P. trichocarpa* sites shown in black triangles and those associated with *P. fremontii* sites shown in red triangles. Locations of groundwater (GW) and soil moisture $\delta^{18}O$ sampling from 2018 to 2019 labeled with pink asterisks. Pixel coloring denotes average number of days with fog cover in June from 2010 to 2019, retrieved from Google Earth Engine (Gorelick et al., 2017). Sources: terrain map from Esri World Terrain Bae (ArcGIS Pro 3.1), floodplain boundaries from Stillwater Sciences (2019), watershed boundary from the National Hydrography Dataset (NHDH_CA), via The National Map.

2.3. Response Variables ($\delta^{18}O$ and $\Delta^{13}C$)

Cores were prepared and annual growth rings were measured, crossdated, and detrended using splines fit to each tree's growth series (Williams et al., 2022). For each of the seven sites, a subset of six trees (42 trees total) with the

Table 1
Site Information for Populus trichocarpa and P. fremontii Trees Sampled Along the Lower Santa Clara River, California

Site	Latitude (°)	Longitude (°)	Elevation (m)	Distance from coast (km)	Mean VPD_{max} (kPa)[a]	Mean DTG (m)[b,c]	Species
Hanson	34.3070	−119.0993	55	17	1.7	3.2	*P. trichocarpa*
South Mountain Road	34.3911	−119.0519	76	23	2.0	2.1	*P. trichocarpa*
Hedrick Ranch Lower	34.3552	−119.0153	88	26	2.0	1.2	*P. trichocarpa*
Hedrick Ranch Upper	34.3569	−119.0111	89	26	2.0	0.7	*P. trichocarpa*
Taylor	34.3644	−118.9921	96	28	2.0	2.2	*P. trichocarpa*
Fillmore Cienega	34.3895	−118.8758	148	40	2.5	5.4	*P. fremontii*
Newhall Ranch	34.4280	−118.6215	299	63	3.1	0.8	*P. fremontii*

[a]Mean maximum vapor pressure deficit (VPD_{max}) was calculated using daily summer (March - September) values from 2010–2019, retrieved from PRISM Climate Group (Oregon State University). [b]Mean depth to groundwater (DTG) was calculated by averaging annual median-values of all observations from 2011–2019. [c]Full time series of DTG for each site can be found in Williams et al. (2022) Figure 4.

Table 2
Correlations Between $\delta^{18}O$ and Environmental Drivers

		Atmospheric drivers[a]		Moisture-related drivers[b]			
Response variable	Months[c]	T_{max} (°C)	VPD_{max} (kPa)	Sc-PDSI	DTG (m)	PPT (mm)	Winter PPT (mm)[d] Prev. Oct- cur. Mar
$\delta^{18}O$ (earlywood)	February–June	0.87***	0.89***	−0.82***	0.82***	−0.61*	−0.45
$\delta^{18}O$ (latewood)	March–September	0.49	0.82***	−0.82***	0.63*	−0.32	−0.72**

Note. $\delta^{18}O$ data were averaged across all trees of both species at all seven sites (42 trees) along the lower Santa Clara River, California. Environmental drivers and response variables were averaged across sites to calculate regional means. Significance codes: $p < 0.1$ (*), $p < 0.05$ (**), $p < 0.01$ (***). [a]Atmospheric drivers: T_{max} = maximum temperature, VPD_{max} = maximum vapor pressure deficit. [b]Moisture-related drivers: sc-PDSI = self-calibrated Palmer Drought Severity Index; DTG = Depth to Groundwater; PPT = precipitation. [c]Annual values for environmental drivers were averaged (summed for precipitation) over the time period noted in the "Months" column. [d]Water-year winter precipitation values were also summed from October of the previous year to March of the current year.

strongest correlation to site-averaged ring-width chronologies was chosen for carbon and oxygen stable isotope analyses. For each tree, 10 annual rings (2010–2019) were selected for isotopic analysis, spanning pre-drought (2010–2011), peak drought (2013–2016), and drought recovery (2017–2019) periods. As described in Williams et al. (2022), annual rings were separated into earlywood and latewood segments and reduced to α-cellulose for a total of 20 samples per tree for carbon and oxygen stable isotope analysis. A description of isotope analyses, precision, and standards is included in Supporting Information S1 (Text S1 and Table S1), and all tree-ring stable carbon and oxygen isotope data used for this study are publicly available (Williams, 2022).

Mass spectrometer measurements of $\delta^{13}C$ were converted to carbon isotope discrimination ($\Delta^{13}C$) to reflect plant-level processes (Farquhar et al., 1989):

$$\Delta^{13}C = \left(\delta^{13}C_{atmosphere} - \delta^{13}C_{plant}\right)/\left(1 - \delta^{13}C_{plant}/1000\right) \quad (1)$$

Smoothed $\delta^{13}C_{atmosphere}$ data were obtained from ScrippsCO_2 station in La Jolla, CA (Keeling et al., 2001).

2.4. Environmental Drivers

Daily climate data, including precipitation (PPT), maximum temperature (T_{max}), and maximum vapor pressure deficit (VPD_{max}) were obtained from PRISM Climate Group at 4 km resolution (Oregon State University; Daly et al., 2008); and monthly self-calibrated Palmer Drought Severity Index (sc-PDSI) data were obtained separately for the same pixels (WestWide Drought Tracker; Abatzoglou et al., 2017; Palmer, 1965). PDSI is a commonly-used drought index that has shown strong correlations with measured growing season soil moisture content (Dai, 2011; Dai et al., 2004; Wang et al., 2015), and its self-calibrated variant (sc-PDSI) accounts for differences in climate regime among pixels to facilitate site comparisons (Wells et al., 2004). Depth to groundwater (DTG) was calculated for each site based on groundwater elevation data from nearby wells obtained from the California Department of Water Resources' California Statewide Groundwater Elevation Monitoring online portal (CDWR SGMA Data Viewer, 2020), as described in Williams et al. (2022).

2.5. Data Analyses

To evaluate the regional response of cottonwood trees in the lower Santa Clara River to environmental drivers, annual values of tree-ring cellulose $\delta^{18}O$ from 2010 to 2019 were averaged across trees from all sites (42 trees), with earlywood and latewood fractions analyzed separately. Correlations were calculated between $\delta^{18}O$ and environmental drivers, which included a mix of atmospheric drivers (T_{max}, and VPD_{max}) and moisture related drivers (PPT, sc-PDSI and DTG). Correlations between $\Delta^{13}C$ and environmental drivers for the same trees and time period can be found in Williams et al. (2022) Table 2. Data for environmental drivers were averaged across sites within each year and aggregated over the early growing season (February–June) for comparison with earlywood $\delta^{18}O$ values, and over the late growing season (March–September) for comparison with latewood $\delta^{18}O$ values. As rain is mostly absent during the summer in this Mediterranean climate and groundwater recharge generally occurs in winter, correlations were also calculated between response variables and water-year winter (previous October - current March) PPT. Because some data did not conform to a normal distribution, all

correlations between $\delta^{18}O$ and environmental drivers were evaluated using the non-parametric Spearman's rank-order correlation.

$\Delta^{13}C$ residuals ($\Delta^{13}C_{res}$) were calculated for each species to account for significant species differences in baseline (pre-drought) $\Delta^{13}C$ values that could obscure interpretations of drought responses, as these baseline differences could be due to physiological (e.g., Sparks & Ehleringer, 1997) or anatomical (e.g., Ponton et al., 2001) species differences unrelated to the environmental drivers evaluated in this study. Values of $\Delta^{13}C_{res}$ were calculated separately for each species as departures from baseline (pre-drought) conditions, which we define as the mean of the 2010–2011 $\Delta^{13}C$ values across all trees within each species. This approach allows for the evaluation of shared species responses to environmental drivers and facilitates the more direct comparison of species differences in drought responses. Specifically, $\Delta^{13}C_{res}$ was calculated by subtracting the mean baseline $\Delta^{13}C$ values of each species from annual $\Delta^{13}C$ values of each tree within their respective species. Therefore, positive $\Delta^{13}C_{res}$ values represent increased ^{13}C discrimination relative to baseline conditions. For trees under high-light conditions in this water-limited system, increased ^{13}C discrimination suggests greater stomatal conductance, usually associated with negligible water limitation. Conversely, negative $\Delta^{13}C_{res}$ values indicate decreased ^{13}C discrimination, suggesting reduced stomatal conductance, which is commonly induced by drought stress in this biome.

To evaluate the influence of evaporative demand on the correlation between carbon and oxygen isotope ratios, Spearman's rank-order correlations were calculated between annual $\delta^{18}O$ and $\Delta^{13}C_{res}$ values across all 42 trees and plotted as a function of annual, site-averaged VPD_{max} for the 2010–2019 period. Correlations were calculated separately for earlywood and latewood isotope values and compared to average early season (February - June) and late season (March - September) VPD_{max}, respectively. Separate linear trendlines were then fit to earlywood and latewood values. Statistical analyses were carried out using R version 4.2.1 (R Core Team, 2022).

To retrospectively infer water sources used by trees included in this study, we employed Sargeant et al. (2019)'s Identification of Source-water Oxygen isotopes in trees Toolkit (ISO-Tool). ISO-Tool applies an inverse of the Barbour et al. (2004) model of biochemical fractionation to estimate source water used by plants based on observed tree-ring $\delta^{18}O$ values, climate inputs, and plant physiological variables, as described in Supporting Information S1 (Text S2, Table S2). We compared the resulting source water $\delta^{18}O$ estimations ($\delta^{18}O_{mod}$) with observed groundwater (shallow well) and soil moisture (20–100 cm depth) $\delta^{18}O$ data collected from three of the study sites (Figure 1) between April 2018 and July 2019 (Figures 5e and 5f; Text S3 and Table S3 in Supporting Information S1). To validate model results, we compared $\delta^{18}O_{mod}$ from 2018–2019 at these three sites with xylem $\delta^{18}O$ data collected by Kui and Kibler (2023) from separate *Populus* spp. trees during the same time period and at the same sites (Text S2 and Figure S2 in Supporting Information S1).

3. Results

3.1. Interannual Trends and Seasonal Patterns in Environmental Drivers and Response Variables

Values of sc-PDSI and VPD_{max} climate data were aggregated across all seven sites to provide a regional context of drought conditions and atmospheric demand during the study period (Figures 2a and 2b). Mean annual sc-PDSI was similar between early and late season (Figure 2a; paired *t*-test: $T_9 = -0.06$, $p = 0.95$), which is expected given the modeled lag in soil moisture incorporated in this drought index. In contrast, VPD_{max} showed significant seasonal differences (paired *t*-test: $T_9 = -14.8$, $p < 0.001$) and was on average 0.4 kPa higher in the late season, which is characteristic of the Mediterranean climate in southern California. During the pre-drought period (2010–2011), average sc-PDSI across sites was 0.36 (mean of early and late season), indicating relatively favorable moisture conditions for the region, and site-averaged VPD_{max} was 1.5 kPa (early season) and 2.0 kPa (late season). Following the onset of the drought in 2012, sc-PDSI declined sharply and remained below −3.7 during the peak of the drought (2013–2016), signifying severe to exceptional drought conditions (Figure 2a). VPD_{max} concurrently increased and reached its most extreme in 2015, at 2.0 kPa (early season) and 2.3 kPa (late season) (Figure 2b). Values of sc-PDSI generally increased during the drought recovery period (2017–2019), coinciding with strong groundwater recharge across sites (Williams et al., 2022). Sc-PDSI experienced a minor decrease in 2018 before rebounding to −0.3 in 2019 (Figure 2a). VPD_{max} steadily declined during the drought recovery period and fell below pre-drought values in 2019, reaching 1.3 kPa (early season) and 1.9 kPa (late season) (Figure 2b). Together, these climate trends depict relatively benign baseline (pre-drought) conditions from 2010–2011, followed by severe water limitation and high atmospheric demand during the peak of the drought (2013–2016), and a gradual return to pre-drought conditions during the drought recovery period (2017–2019).

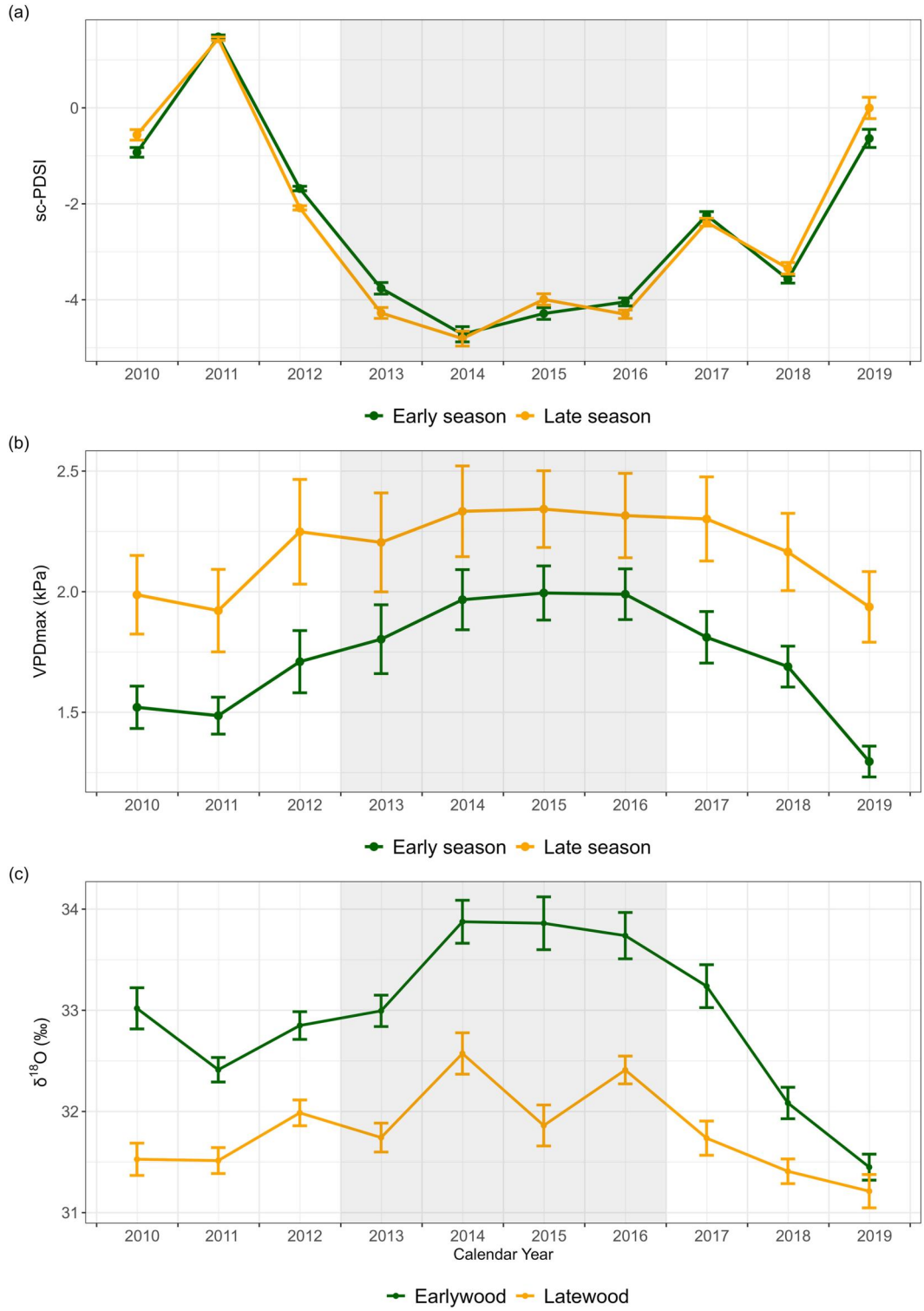

Figure 2. (a) Time series of self-calibrated Palmer Drought Severity Index (sc-PDSI), averaged across all seven sites within the lower Santa Clara River, California. Climate data were aggregated over the early season (February–June) to coincide with tree earlywood production (green), and late growing season (March–September) to coincide with tree latewood production (orange). (b) Time series of maximum vapor pressure deficit (VPD_{max}) during the early growing season (green) and late growing season (orange), averaged across all sites. (c) Regional isotope dendrochronologies of $\delta^{18}O$ in earlywood (green) and latewood (orange) averaged across trees of both species from all seven sites (42 trees total). Bars display ±1SE. Gray shading denotes the peak drought period (2013–2016).

$\delta^{18}O$ data from both species were combined across trees from all seven sites (42 trees total) to evaluate common responses of cottonwoods to environmental drivers within the lower Santa Clara River and for comparison with the regionally-averaged $\Delta^{13}C$ presented for the same trees and time period in Williams et al. (2022) and reproduced in Figure S3 in Supporting Information S1. $\Delta^{13}C$ and $\delta^{18}O$ were highly responsive to drought conditions, with interannual trends of $\Delta^{13}C$ most closely following those of PDSI (Williams et al., 2022; Figure S3 in Supporting Information S1), and those of $\delta^{18}O$ more strongly mirroring VPD_{max} (Figures 2b and 2c). Both earlywood and latewood $\delta^{18}O$ exhibited strong enrichment from their pre-drought averages (32.7 and 31.5‰, respectively), reaching their highest point during the peak of the drought, in 2014 (33.9 and 32.6‰). Values of $\delta^{18}O$ showed a marked decline during the drought recovery period, with the most depleted values of the study period observed in 2019 (31.4 and 31.2‰).

While interannual trends in $\delta^{18}O$ were positively related to changes in VPD_{max}, we observed pronounced seasonal differences in $\delta^{18}O$ that ran counter to the expected climate response; $\delta^{18}O$ was consistently lower in latewood of every year, despite VPD_{max} being significantly higher in the late season (Figures 2b and 2c). In fact, the average difference between annual earlywood and latewood $\delta^{18}O$ (−1.2‰) was more than double the average annual change between sequential years in either earlywood (0.5‰) or latewood (0.4‰). The fact that seasonal changes in $\delta^{18}O$ were greater than interannual changes, and in an opposing response to VPD_{max}, indicates that the consistent intra-annual decrease in $\delta^{18}O$ is unlikely attributable to seasonal shifts in atmospheric conditions (Figures 2b and 2c).

3.2. Correlations Between Environmental Drivers and Response Variables

In prior work, we established that the trees included in this study showed strong and significant correlations between carbon isotope discrimination ($\Delta^{13}C$) and nearly all environmental drivers, with the strongest ($p < 0.01$) relationships for DTG ($r < -0.9$), T_{max} ($r < -0.85$), and VPD_{max} ($r < -0.83$) (Williams et al., 2022). For oxygen isotopes, there were also significant relationships with these environmental variables, but the correlations varied seasonally, with earlywood $\delta^{18}O$ generally more sensitive to hydroclimate drivers than latewood (Table 2). The strongest relationship was between earlywood $\delta^{18}O$ and VPD_{max} ($r = 0.89$), with latewood only slightly less correlated ($r = 0.82$). Similarly, DTG was linked positively and significantly with $\delta^{18}O$, and the earlywood correlation ($r = 0.82$) was stronger than latewood ($r = 0.63$). The most notable seasonal differences in $\delta^{18}O$ correlations were observed for temperature and precipitation (Table 2). T_{max} was significantly correlated with earlywood $\delta^{18}O$ ($r = 0.87$), but not with latewood. Precipitation showed opposite seasonal relationships with $\delta^{18}O$; earlywood was significantly correlated only with current-year (February–June) precipitation ($r = -0.61$), and latewood significantly correlated ($r = -0.72$) only with prior winter precipitation (prev. Oct–cur. March). Notably, winter precipitation is largely responsible for the bulk of annual groundwater recharge in this system. Together these relationships indicate that water availability and atmospheric demand had a combined influence on both $\delta^{18}O$ and $\Delta^{13}C$, but that seasonal differences in climate sensitivity were more pronounced for $\delta^{18}O$.

Of all atmospheric drivers, VPD_{max} exhibited the strongest combined correlations with both $\delta^{18}O$ and $\Delta^{13}C$ (Table 2; Williams et al., 2022: Table 2), suggesting a set of similar physiological mechanisms by which atmospheric dryness influenced both proxies. Although earlywood $\delta^{18}O$ and $\Delta^{13}C$ were both significantly correlated with VPD_{max} on an interannual basis, the coordinated physiological response of trees to VPD_{max} (via correlations between carbon and oxygen isotopes across individuals in the same year) was lower in earlywood compared to latewood (Figure 3). In fact, there were no years when $\delta^{18}O$ and $\Delta^{13}C_{res}$ were significantly correlated across all 42 trees for earlywood (Figure 3). In contrast, isotopic coordination was strongly related to VPD_{max} in the late season, when VPD_{max} was 0.4 kPa higher, on average. In years with higher late-season VPD_{max}, latewood $\delta^{18}O$ and $\Delta^{13}C_{res}$ values among all trees showed stronger (negative) correlations, indicating a more pronounced coordinated response of these variables with greater evaporative demand (Figure 3).

3.3. Species Differences in Response Variables and Apparent Water-Use Strategies

We observed apparent differences between *P. trichocarpa* and *P. fremontii* in their water-use strategies and drought responses, demonstrated by: (a) contrasts in $\delta^{18}O$ and $\Delta^{13}C$ values before the drought (Figure 4); (b) the magnitude of their change from baseline values during the drought; and (c) the immediacy of their drought response and recovery (Figures 5a and 5b). In pre-drought years (2010–2011), *P. fremontii* had significantly

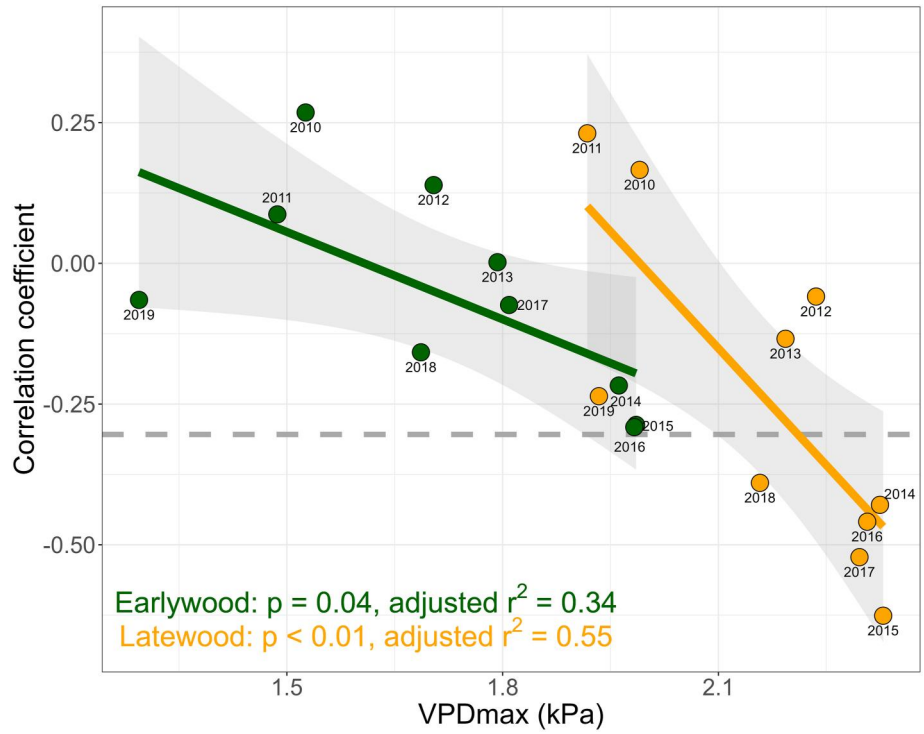

Figure 3. Correlations between annual values of $\delta^{18}O$ and $\Delta^{13}C$ residuals ($\Delta^{13}C_{res}$) as a function of maximum vapor pressure deficit (VPD_{max}). Pairs of $\Delta^{13}C_{res}$ and $\delta^{18}O$ values for all trees at all sites within the lower Santa Clara River, California (42 trees) were compared to calculate annual values of correlation, with each point representing a year from 2010 to 2019. Correlations were calculated separately for earlywood (green) and latewood (orange). Values of VPD_{max} were aggregated across all sites and averaged over the months of February–June for the earlywood comparison and March–September for the latewood comparison. Separate trendlines are displayed for earlywood and latewood with standard error shaded. Horizontal dashed line depicts the threshold below which all points show a significant correlation between $\Delta^{13}C_{res}$ and $\delta^{18}O$ ($p < 0.05$).

higher $\Delta^{13}C$ for both earlywood (Welch's *t*-test, $t_{21} = 6.20$, $p < 0.001$) and latewood (Welch's *t*-test, $t_{27} = 7.78$, $p < 0.001$) by an average of 1.9‰ (mean of earlywood and latewood), indicating higher C_i/C_a for this species under relatively non-stressed conditions (Figures 4a and 4b). During this same time period, earlywood $\delta^{18}O$ was similar between species (Welch's *t*-test, $t_{26} = -0.36$, $p = 0.72$), while latewood $\delta^{18}O$ of *P. fremontii* was slightly, but significantly, depleted compared to *P. trichocarpa* (Welch's *t*-test, $t_{26} = -2.31$, $p = 0.03$) by an average of 0.5‰ (Figures 4c and 4d).

As the drought began, *P. trichocarpa* showed a gradual decrease in $\Delta^{13}C_{res}$ that did not exceed 0.5‰ per year (Figure 5a). In contrast, $\Delta^{13}C_{res}$ for *P. fremontii* trees remained at pre-drought levels (2010–2011) through 2013, until experiencing a precipitous decline of 2.1‰ (mean of earlywood and latewood) in 2014 (Figure 5b). The recovery of *P. fremontii* was similarly more dynamic than that of *P. trichocarpa*, where mean $\Delta^{13}C_{res}$ began to increase (+0.5‰) in 2015 for *P. fremontii* but continued to decline until 2016 for *P. trichocarpa*. Together, these results indicate a more delayed but severe regulation of leaf gas-exchange for *P. fremontii*.

Modeled estimates of source water $\delta^{18}O$ ($\delta^{18}O_{mod}$) revealed a shared seasonal pattern of source water shifting, as well as species differences in water sources. Latewood $\delta^{18}O_{mod}$ was consistently depleted relative to earlywood, indicating that both species shifted toward the use of more depleted moisture sources in the late season. In this system, groundwater $\delta^{18}O$ is more depleted (mean = −7.3‰ ± 0.6‰ SD) than soil moisture (−4.0‰ ± 3.4‰) (Table S3 in Supporting Information S1), and generally closer to the range of latewood $\delta^{18}O_{mod}$, suggesting that trees used a greater proportion of groundwater in late season (Figures 5e and 5f). In addition, the variation among years for latewood $\delta^{18}O_{mod}$ values was smaller than earlywood in both *P. trichocarpa* (1.2‰ latewood vs. 2.6‰ earlywood) and *P. fremontii* (2.8‰ latewood vs. 4.0‰ earlywood), as would be expected with more consistent consumption of deeper water sources in the late season.

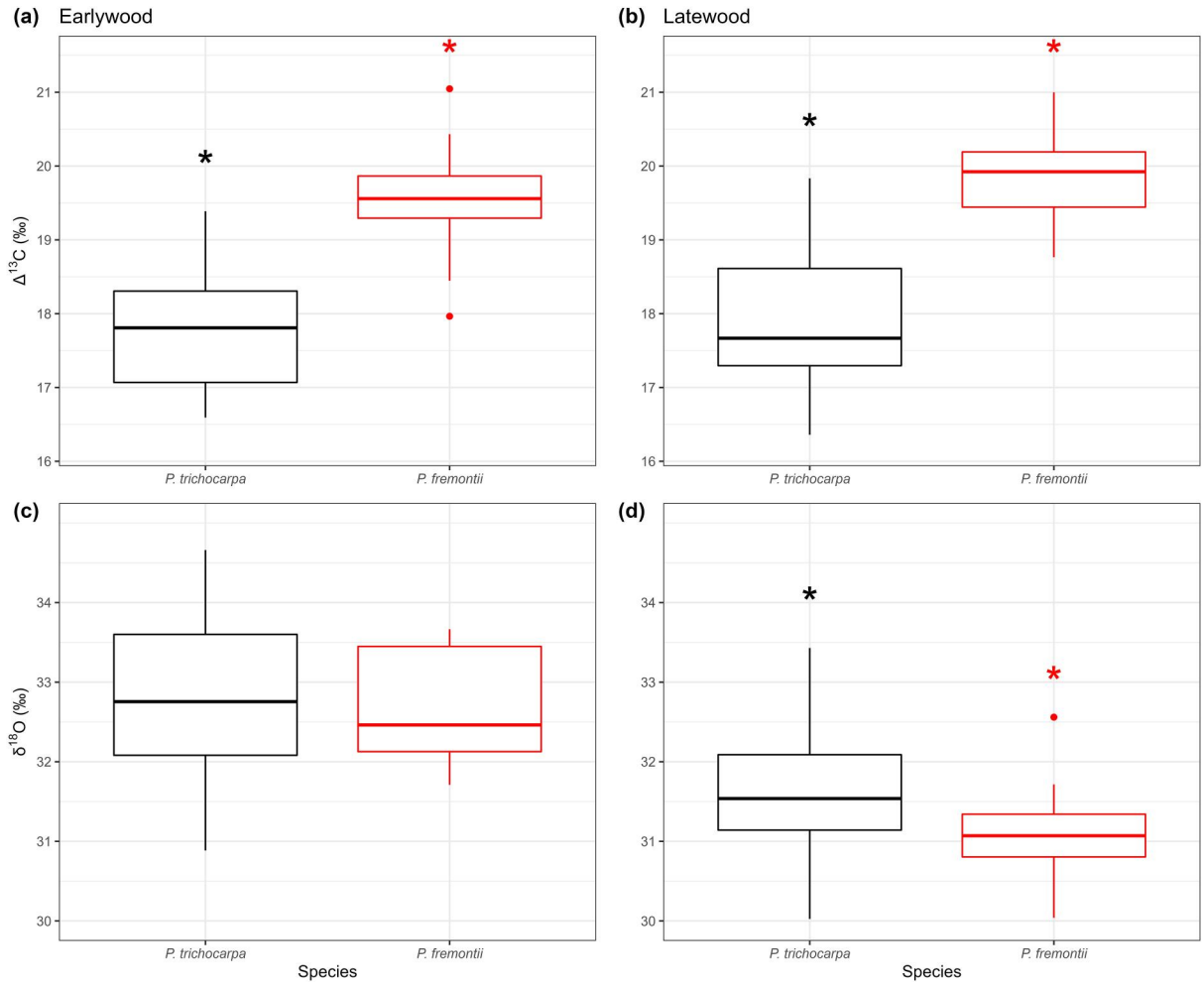

Figure 4. Boxplots depicting mean pre-drought (2010–2011) values of response variables ($\delta^{18}O$ and $\Delta^{13}C$) for all trees of each species (30 *P. trichocarpa* and 12 *P. fremontii*). Boxplots were calculated separately for earlywood (a) and (b) and latewood (c) and (d). Asterisks denote significant differences between species as determined by Welch's two-sample *t*-tests ($p < 0.05$).

Comparing the two species, *P. fremontii* exhibited consistently lower $\delta^{18}O_{mod}$ than *P. trichocarpa*, by an average of −1.9‰ (mean of earlywood and latewood), and *P. fremontii* earlywood $\delta^{18}O_{mod}$ even overlapped with the observed groundwater signal in some years (Figure 5f). In contrast, $\delta^{18}O_{mod}$ of *P. trichocarpa* was consistently more enriched than the groundwater signal in earlywood of every year, and also in latewood of some years (Figure 5e). Together these source water estimates indicate that both species shifted toward the use of more depleted water sources over the growing season, but that *P. fremontii* used proportionally more depleted water sources.

4. Discussion

An important finding of this study was the seasonal and species-level variation in groundwater dependence for riparian cottonwoods, which are foundation species in dryland ecosystems (Patten, 1998; Stromberg, 1993). We applied tree-ring stable isotopes in a novel context to evaluate the timing and drivers of tree ecophysiological function, as well as their vulnerability to drought and climate change. By analyzing early and late season oxygen and carbon stable isotopes in tree rings separately and in a dual-isotope approach, we were able to resolve key temporal strategies that varied by species for accessing more depleted (deeper) water sources to mitigate atmospheric drought conditions and soil-moisture limitation. Our results revealed cottonwoods in this system to be facultative phreatophytes that used shallow soil moisture advantageously but relied on deeper moisture sources to maintain physiological function during seasonally dry conditions and long-term drought. By comparing species

10.1029/2023WR035928

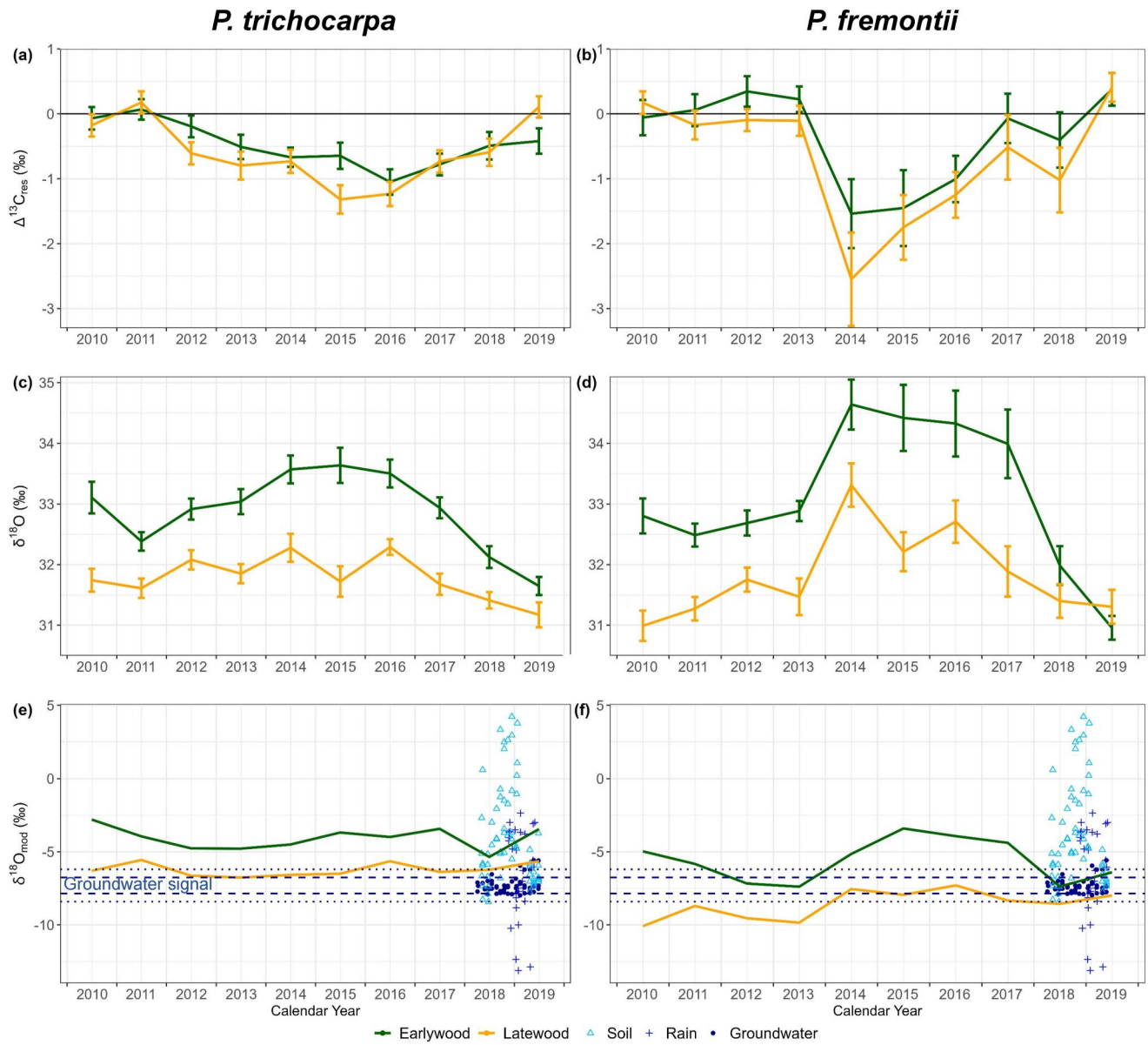

Figure 5. Species-level responses for *Populus trichocarpa* trees ($n = 30$) at five sites (panels a, c, e) and *P. fremontii* trees ($n = 12$) at two sites (panels b, d, f) along the lower Santa Clara River, California. Panels (a) and (b): isotope dendrochronologies of earlywood $\Delta^{13}C$ residuals ($\Delta^{13}C_{res}$; green) and latewood $\Delta^{13}C_{res}$ (orange) averaged across all trees within each species. Bars display ±1 SE. Panels (c) and (d): isotope dendrochronologies of earlywood $\delta^{18}O$ (green) and latewood $\delta^{18}O$ (orange) cellulose averaged across all trees within each species. Panels (e) and (f): modeled source water $\delta^{18}O$ ($\delta^{18}O_{mod}$) for earlywood (green) and latewood (orange) calculated as a single mean value for each site and averaged across all sites containing each species. Points in panels (e) and (f) denote soil moisture (20–100 cm depth), rain, and groundwater $\delta^{18}O$ observations. Blue dashed lines in panels (e) and (f) denote the mean of groundwater $\delta^{18}O$ observations ±1 SD, and dotted lines denote ±2 SD (Table S3 in Supporting Information S1).

with overlapping distributions across a pronounced aridity gradient, our results provide implications as to how increasingly severe droughts and warmer temperatures associated with climate change may differentially affect the distribution and survival of each species.

4.1. Seasonal Shifts in Groundwater Dependence

We observed a distinct seasonal pattern in $\delta^{18}O$ that suggests trees shifted water sources over the course of the growing season. As expected, both earlywood and latewood $\delta^{18}O$ were significantly positively correlated with VPD_{max} in their respective seasons (Table 2) and shared the same interannual trends (Figures 2b and 2c).

However, we observed seasonal changes in $\delta^{18}O$ that were surprisingly opposite that of VPD_{max}; latewood $\delta^{18}O$ was significantly depleted relative to earlywood in nearly every year despite VPD_{max} being significantly higher in the late season of every year (Figures 2b and 2c). The magnitude of seasonal shifts in $\delta^{18}O$ were, on average, more than double the interannual variation for either earlywood or latewood alone, suggesting a stronger mechanism driving intra-annual changes in $\delta^{18}O$. Studies have shown that changes in source water can exert greater control over the $\delta^{18}O$ signature of tree-ring cellulose than leaf (or needle) water enrichment and can effectively overshadow the leaf water signature (Barbour et al., 2004; Sarris et al., 2013; Treydte et al., 2014). Analogously here, the $\delta^{18}O$ data suggest that interannual trends were largely reflective of changes in leaf water enrichment in response to fluctuating atmospheric conditions, but the pronounced and consistent seasonal shift to more depleted $\delta^{18}O$ likely resulted from trees utilizing water in deeper soil layers late in the growing season when soil moisture in the vadose zone was scarce. Within dryland systems, deep soil moisture is generally supported by groundwater via the capillary fringe that links saturated and unsaturated soil layers (Camporeale et al., 2019), hence the seasonal use of more depleted source waters indicates a reliance on groundwater to maintain physiological function during summer drought. Source water modeling results further support these inferences as earlywood $\delta^{18}O_{mod}$ was enriched relative to groundwater in most years, and latewood $\delta^{18}O_{mod}$ was close to, or within, the range of observed groundwater $\delta^{18}O$ in every year (Figures 5e and 5f).

Our observations are consistent with similar accounts of plants increasing groundwater use seasonally in semi-arid and Mediterranean climates, where precipitation is strongly limiting during the growing season (Antunes et al., 2018; Barbeta et al., 2015; Eggemeyer et al., 2008; Mayes et al., 2020; Phelan et al., 2022; Snyder & Williams, 2000; Voltas et al., 2015; Zimmerman et al., 2023). Many species that inhabit these systems exhibit dimorphic root systems (both shallow, lateral roots and deep taproots), allowing them to exploit seasonal differences in water and nutrient availability (Antunes et al., 2018; Dawson & Pate, 1996; Snyder & Williams, 2000). Even with perennial groundwater availability, it may be advantageous for plants to maintain shallow lateral roots to exploit the higher nutrient concentrations that are characteristic of shallow soil layers (Evans & Ehleringer, 1994; Gebauer & Ehleringer, 2000), especially considering that these nutrients may not be labile and thus unavailable later in the growing season when soil moisture is scarce. Conversely, trees may also need to use a considerable portion of groundwater even when soil moisture is available in cases when high evaporative demand increases tree water requirements (Flanagan et al., 2019). Thus, shifting source water over the course of the growing season may increase the survival and productivity of riparian phreatophytes in dryland regions.

4.2. Greater Coordination of $\delta^{18}O$ and $\Delta^{13}C$ Responses With Increased Atmospheric Demand

Annual comparisons of $\delta^{18}O$ and $\Delta^{13}C_{res}$ correlations across trees from all sites revealed a coordinated response to changes in VPD_{max} (Figure 3). Evaporative demand strongly influences stomatal conductance, which in turn mediates leaf water enrichment and leaf internal CO_2 concentration. Consequently, VPD_{max} (i.e., evaporative demand) should exert strong control over both $\delta^{18}O$ and $\Delta^{13}C$ when stomatal conductance is the primary mechanism influencing these variables. Consistent with this reasoning, $\delta^{18}O$ and $\Delta^{13}C_{res}$ showed stronger correlations in years with higher VPD_{max}, and this relationship was more pronounced in the late growing season, when significantly higher VPD_{max} would presumably induce a stronger stomatal response (Figure 3). Interestingly, Guo et al. (2022) showed that stomatal conductance of *P. fremontii* along the arid San Pedro River in Arizona was largely unresponsive to changes in VPD under favorable water status (i.e., DTG <1 m). We found that many of the years with the strongest correlations between $\delta^{18}O$ and $\Delta^{13}C_{res}$ occurred during the peak of the drought and in its immediate aftermath. This pattern suggests that water limitation increased the stomatal sensitivity of trees to VPD_{max}, as plants may demonstrate differential responses to changes in evaporative demand based on their water status (Williams et al., 2022).

The less coordinated response of earlywood $\delta^{18}O$ and $\Delta^{13}C_{res}$ to changes in atmospheric demand (Figure 3) could also be the result of post-photosynthetic processes or seasonal differences in source water. In a recent review, Siegwolf et al. (2023) note the potential for reallocation of stored carbohydrates to contribute to a dampening effect on ^{13}C that could obscure dual isotope ($\delta^{18}O$ and $\Delta^{13}C$) interpretations in earlywood. In addition, the early season use of shallow soil moisture, which is more isotopically variable, may have overshadowed the influence of leaf water enrichment and resulted in a partial decoupling of tree-ring $\delta^{18}O$ and stomatal conductance. Sargeant and Singer (2016) showed that the $\delta^{18}O$ of tree-ring cellulose exhibited greater variability when *P. nigra* trees used shallow soil moisture compared to groundwater, which had a more consistent isotopic composition. Therefore, the greater use of deeper (and more isotopically stable) moisture sources during the hot, dry summer

likely resulted in a more consistent $\delta^{18}O$ signal of source water and allowed for a more coordinated response of $\Delta^{13}C_{res}$ and $\delta^{18}O$ that reflected leaf-level processes. Furthermore, greater drought stress during the late season could similarly reduce the influence of source water relative to leaf-level enrichment, as stomatal closure weakens the Péclet effect (Siegwolf et al., 2023). In this context, our interpretations are consistent with assumptions and predictions under the dual isotope approach of Scheidegger et al. (2000), in which concurrent enrichment of $\delta^{18}O$ and reduction of $\Delta^{13}C$ under increasing VPD_{max} signify reductions in stomatal conductance (as opposed to directional changes in net photosynthesis).

4.3. Species Differences in Water Sources

Species differences in groundwater reliance are consistent with their distributions along the Santa Clara River, with *P. trichocarpa* found in cooler coastal reaches and *P. fremontii* in more arid inland reaches (Orr et al., 2011). Source water modeling suggests that *P. fremontii* utilized shallow moisture sources early in the growing season, but relied on groundwater as its main water source during dry summer months (Figure 5f). *P. fremontii* is generally distributed in low-lying floodplains of more arid regions with historically shallow and stable water tables, which promotes high groundwater reliance for this species (Hultine et al., 2020; Rood et al., 2003). However, previous studies from Arizona (USA) indicate that the extent of such groundwater reliance varies with hydroclimatic conditions. For example, along the perennial Bill Williams River, which regularly experiences extreme summer temperatures, Busch et al. (1992) showed that *P. fremontii* relied almost exclusively on groundwater to facilitate high transpiration, ostensibly as a means of canopy cooling. In contrast, Snyder and Williams (2000) found that *P. fremontii* along an intermittent segment of the San Pedro River predominately consumed groundwater but advantageously sourced 33% of its xylem water from soil moisture following summer monsoon rains. This latter observation is more similar to our own findings, where greater water table variability and less extreme temperatures compared to the Bill Williams River encouraged *P. fremontii* to rely on groundwater during seasonal drought, but advantageously use shallower moisture sources when available. *P. trichocarpa* also shifted toward the use of more depleted source water during summer drought, but $\delta^{18}O_{mod}$ suggests this species used a lesser proportion of groundwater compared to *P. fremontii*. *P. trichocarpa* is commonly found in more temperate regions (Rood et al., 2003), where milder temperatures facilitate lower water requirements. Hence, *P. trichocarpa* may use a lesser proportion of groundwater due to hydroclimatic adaptations that confine its distribution to cooler, more coastal reaches of the Santa Clara River (Orr et al., 2011). However, both species shifted toward the use of deeper (groundwater-supported) moisture sources to mitigate drought conditions, implying a shared susceptibility to forecasted trends of long-term groundwater decline in dryland regions (Ghazavi & Ebrahimi, 2018; Hanson et al., 2012).

Some *P. fremontii* values of $\delta^{18}O_{mod}$ were more depleted than the groundwater $\delta^{18}O$ signal observed in 2018 and 2019 (the only years for which concurrent field data were available; Figure 5f), which could be due to spatial and/or temporal heterogeneity of $\delta^{18}O$ in precipitation and groundwater throughout the floodplain. The combination of continental and elevation effects on isotopes in rain water (Dutton et al., 2005) could presumably generate more depleted source water $\delta^{18}O$ at *P. fremontii* sites, which are upstream (further inland) and higher in elevation than *P. trichocarpa* sites. Furthermore, we observed precipitation $\delta^{18}O$ to be highly variable and more depleted than the groundwater signal by nearly 5‰ during some rain events from 2018–2019 (Figures 5e and 5f), highlighting the possibility of interannual variability in $\delta^{18}O$ of precipitation-driven groundwater recharge (Figures 5e and 5f). Alternatively, this observation could be the result of greater post-photosynthetic oxygen exchange in *P. fremontii* than accounted for in source water modeling, which was hypothesized by Stolar (2019) but to our knowledge has not been documented. Nevertheless, the consistency between $\delta^{18}O_{mod}$ values at the Fillmore Cienega site from 2018–2019 and separate measurements of cottonwood xylem $\delta^{18}O$ at the same site and time period provide support for source water modeling results (Figure S2 in Supporting Information S1).

4.4. Species Differences in Leaf Gas-Exchange and Drought Response

P. fremontii exhibited significantly higher $\Delta^{13}C$ than *P. trichocarpa* during both the pre-drought (Figure 4) and drought recovery periods (Welch's *t*-tests, $t_{20} > 4.79$, $p < 0.001$), which could be due to physiological or anatomical species differences related to their distributions along the river. For example, unlike *P. trichocarpa* leaves which contain little to no adaxial stomata (Al Afas et al., 2006; Ferris et al., 2002), the leaves of *P. fremontii* have stomata on both the adaxial and abaxial surfaces (Blasini et al., 2022). This adaptation reduces constraints on leaf gas-exchange to allow for heat dissipation and may also increase C_i/C_a (Drake et al., 2019) and consequently

increase carbon isotope discrimination (Bradford et al., 1983). Furthermore, research has shown that a multitude of traits related to leaf gas-exchange (stomatal conductance, transpiration, sapwood area, specific leaf area, etc.) are highly variable for *P. fremontii* and influenced by local climate conditions, with populations in more arid regions displaying traits that facilitate greater leaf gas-exchange (Blasini et al., 2022) that could also influence $\Delta^{13}C$. However, leaf-level comparisons of $\Delta^{13}C$ mechanisms between these species are not available, precluding the determination of whether this contrast is the result of morphophysiological differences, or a consequence of unrelated post-photosynthetic processes (Gessler et al., 2014).

P. fremontii maintained $\Delta^{13}C$ at pre-drought levels even as drought conditions worsened, up until 2014 when trees experienced a precipitous reduction in $\Delta^{13}C$ (Figure 5b) concurrent with a period of accelerating groundwater decline (Williams et al., 2022). This indicates that trees were resistant to moderating leaf gas-exchange rates during the onset of drought stress, which illustrates a water-use strategy whereby trees prioritized maintaining photosynthetic processes over hydraulic safety. Alternatively, *P. fremontii* may have exhibited a delayed drought response due to other factors, such as stronger xylem structure or more extensive rooting architecture than *P. trichocarpa*, that allowed this species to tolerate dry conditions for longer before succumbing to drought stress. Previous studies have demonstrated that *P. fremontii* exhibits minimal stomatal regulation, operates under a narrow hydraulic safety margin, and is highly vulnerable to xylem cavitation (Leffler et al., 2000; Pockman & Sperry, 2000). Our findings demonstrate that sampled (surviving) *P. fremontii* trees in this study did strongly regulate stomatal conductance to prevent water loss at a certain threshold of drought stress (Figure 5b). Yet, the timing of the precipitous reduction in $\Delta^{13}C$ for *P. fremontii* trees also corresponded with sharp increases in mortality for other trees in these stands (including *P. fremontii*) during the same period due to groundwater decline (Kibler et al., 2021), highlighting the risks associated with such a delayed drought response. Interestingly, mean $\Delta^{13}C$ of *P. fremontii* sampled for this study began to recover in 2015, coincident with the peak die-off (Kibler et al., 2021), which could be due to surviving trees experiencing a combination of leaf shedding and branch die-back that increased their root:shoot ratio and allowed them to regain favorable water status, as has been observed for *P. fremontii* in other systems (Rood et al., 2000); this was supported by field evidence of crown die-back for sampled trees (Text S4 and Figure S4 in Supporting Information S1).

P. trichocarpa showed an earlier and more gradual stomatal response to drought stress compared to *P. fremontii* (Figures 5a and 5b). Furthermore, *P. trichocarpa* trees maintained low $\Delta^{13}C$ values throughout the peak of the drought (Figure 5a), indicating water limitation induced persistently higher water-use efficiency (Gornall & Guy, 2007). This conservative strategy may be necessary for *P. trichocarpa* in dryland regions, considering this species is also highly vulnerable to xylem cavitation (Fichot et al., 2015). In line with this reasoning, Bassman and Zwier (1991) found stomatal regulation of *P. trichocarpa* clones in Washington that were subjected to experimental drought to be highly variable and influenced by their climate of origin. In that study, dry-adapted clones exhibited high water use efficiency and stomatal sensitivity in response to declining stem water potential, whereas moist-adapted clones maintained high stomatal conductance despite increasing soil water deficits. Schulte et al. (1987) similarly observed stomatal regulation of *P. trichocarpa* to be conditioned by previous exposure to water limitation. Therefore, in the semi-arid climate of the Santa Clara River, *P. trichocarpa* may have adapted greater stomatal sensitivity to limit transpirational water loss as a drought avoidance strategy. *P. trichocarpa* also exhibited stronger negative $\Delta^{13}C$ correlation with T_{max} and VPD_{max} compared to *P. fremontii* (Table S4 in Supporting Information S1), indicating greater stomatal sensitivity to these environmental drivers. However, stomatal closure can lead to higher internal leaf temperatures (Blasini et al., 2022; Kibler et al., 2023) and consequently increase susceptibility to heat stress (Lipiec et al., 2013; Teskey et al., 2015). Therefore, the tendency of *P. trichocarpa* to close stomata early in response to water limitation may confer greater drought avoidance (Martin-StPaul et al., 2017) while ultimately precluding its establishment in warmer (inland) segments of the river, where it would be even more susceptible to temperature increases anticipated with climate change.

5. Conclusions

Our results demonstrate that riparian cottonwoods in this system were generally facultative phreatophytes that used shallow soil moisture advantageously but shifted toward deeper water sources (i.e., groundwater) when soil moisture was limiting and when increased water consumption was required to meet greater atmospheric demand. We observed clear species differences in water-use strategies and drought responses related to their distribution along the Santa Clara River. *P. trichocarpa* was confined to milder coastal reaches, and *P. fremontii* inhabited more arid river segments, where higher atmospheric demand encouraged greater groundwater reliance. In

response to drought, *P. trichocarpa* moderated leaf gas-exchange earlier to increase water-use efficiency, whereas *P. fremontii* exhibited a more delayed stomatal response and prioritized maintaining physiological function, until a critical point. The greater water-use efficiency of *P. trichocarpa* likely allowed trees to limit water loss, while increasing the risk of carbon limitation and heat stress. In contrast, the more delayed stomatal response of *P. fremontii* likely helped tolerate greater evaporative demand, while increasing its groundwater reliance. The contrasting water-use strategies and drought responses of these species imply that hydroclimatic stressors associated with climate change may differentially affect their persistence and regional range limits. Our findings suggest that the greater groundwater reliance and more arid distribution of *P. fremontii* may increase its susceptibility to severe drought-induced groundwater decline, whereas *P. trichocarpa* may become progressively limited in range due to climate warming.

Conflict of Interest

The authors declare no conflicts of interest relevant to this study.

Data Availability Statement

The data on which this article is based are available in Williams (2022) and Kui and Kibler (2023).

Acknowledgments
Support for this work came from the National Science Foundation-NSF [BCS-1660490, EAR-1700517, and EAR-1700555], the U.S. Department of Defense's Strategic Environmental Research and Development Program-SERDP [RC18-1006], and the Edna Bailey Sussman Fund. Property access was provided by The Nature Conservancy, Newhall Ranch, and Sanger Hedrick. We thank Drs. Chris Kibler and Melissa Rohde for project guidance. We thank Chuck Schirmer and Drs. Katie Becklin, Brian Leydet, and Hyatt Green for providing laboratory space, equipment, and logistical support. Finally, we thank Alan Espinoza and Sean Carey for assisting with fieldwork. Any use of trade, firm or product names is for descriptive purposes only and does not imply endorsement by the U.S. Government.

References

Abatzoglou, J. T., McEvoy, D. J., & Redmond, K. T. (2017). The west wide drought tracker: Drought monitoring at fine spatial scales. *Bulletin of the American Meteorological Society*, *98*(9), 1815–1820. https://doi.org/10.1175/BAMS-D-16-0193.1

Al Afas, N., Marron, N., & Ceulemans, R. (2006). Clonal variation in stomatal characteristics related to biomass production of 12 poplar (Populus) clones in a short rotation coppice culture. *Environmental and Experimental Botany*, *58*(1–3), 279–286. https://doi.org/10.1016/j.envexpbot.2005.09.003

Altieri, S., Mereu, S., Cherubini, P., Castaldi, S., Sirignano, C., Lubritto, C., & Battipaglia, G. (2015). Tree-ring carbon and oxygen isotopes indicate different water use strategies in three Mediterranean shrubs at Capo Caccia (Sardinia, Italy). *Trees*, *29*(5), 1593–1603. https://doi.org/10.1007/s00468-015-1242-z

Andersen, D. C. (2016). Climate, streamflow, and legacy effects on growth of riparian Populus angustifolia in the arid San Luis Valley, Colorado. *Journal of Arid Environments*, *134*, 104–121. https://doi.org/10.1016/j.jaridenv.2016.07.005

Andrews, E. D., Antweiler, R. C., Neiman, P. J., & Ralph, F. M. (2004). Influence of ENSO on flood frequency along the California coast. *Journal of Climate*, *17*(2), 337–348. https://doi.org/10.1175/1520-0442(2004)017<0337:IOEOFF>2.0.CO;2

Antunes, C., Chozas, S., West, J., Zunzunegui, M., Diaz Barradas, M. C., Vieira, S., & Máguas, C. (2018). Groundwater drawdown drives ecophysiological adjustments of woody vegetation in a semi-arid coastal ecosystem. *Global Change Biology*, *24*(10), 4894–4908. https://doi.org/10.1111/gcb.14403

Barbeta, A., Mejía-Chang, M., Ogaya, R., Voltas, J., Dawson, T. E., & Peñuelas, J. (2015). The combined effects of a long-term experimental drought and an extreme drought on the use of plant-water sources in a Mediterranean forest. *Global Change Biology*, *21*(3), 1213–1225. https://doi.org/10.1111/gcb.12785

Barbour, M. M. (2007). Stable oxygen isotope composition of plant tissue: A review. *Functional Plant Biology*, *34*(2), 83. https://doi.org/10.1071/FP06228

Barbour, M. M., & Farquhar, G. D. (2000). Relative humidity-and ABA-induced variation in carbon and oxygen isotope ratios of cotton leaves. *Plant, Cell and Environment*, *23*(5), 473–485. https://doi.org/10.1046/j.1365-3040.2000.00575.x

Barbour, M. M., Roden, J. S., Farquhar, G. D., & Ehleringer, J. R. (2004). Expressing leaf water and cellulose oxygen isotope ratios as enrichment above source water reveals evidence of a Péclet effect. *Oecologia*, *138*(3), 426–435. https://doi.org/10.1007/s00442-003-1449-3

Bassman, J. H., & Zwier, J. C. (1991). Gas exchange characteristics of Populus trichocarpa, Populus deltoides and Populus trichocarpa× P. deltoides clones. *Tree Physiology*, *8*(2), 145–159. https://doi.org/10.1093/treephys/8.2.145

Bateman, H. L., & Merritt, D. M. (2020). Complex riparian habitats predict reptile and amphibian diversity. *Global Ecology and Conservation*, *22*, e0095740. https://doi.org/10.1016/j.gecco.2020.e00957

Battipaglia, G., & Cherubini, P. (2022). Stable isotopes in tree rings of mediterranean forests. In *Stable isotopes in tree rings: Inferring physiological, climatic and environmental responses*. In *Tree physiology* (Vol. 8, pp. 605–629). Springer International Publishing. https://doi.org/10.1007/978-3-030-92698-4

Beller, E. E., Downs, P. W., Grossinger, R. M., Orr, B. K., & Salomon, M. N. (2016). From past patterns to future potential: Using historical ecology to inform river restoration on an intermittent California river. *Landscape Ecology*, *31*(3), 581–600. https://doi.org/10.1007/s10980-015-0264-7

Bennett, S. K., Lambert, A. M., Carey, S. P., & Braman, C. A. (2022). Evaluating pole cutting survival and growth for riparian forest restoration during invasion by polyphagous shot hole borer. *Restoration Ecology*, *30*(5), e13578. https://doi.org/10.1111/rec.13578

Birosik, S. (2006). *State of the watershed - Report on surface water quality in the Santa Clara River watershed*. California Regional Water Quality Control Board - Los Angeles Region.

Blasini, D. E., Koepke, D. F., Bush, S. E., Allan, G. J., Gehring, C. A., Whitham, T. G., et al. (2022). Tradeoffs between leaf cooling and hydraulic safety in a dominant arid land riparian tree species. *Plant, Cell and Environment*, *45*(6), 1664–1681. https://doi.org/10.1111/pce.14292

Braatne, J. H., Jamieson, R., Gill, K. M., & Rood, S. B. (2007). Instream flows and the decline of riparian cottonwoods along the Yakima River, Washington, USA. *River Research and Applications*, *23*(3), 247–267. https://doi.org/10.1002/rra.978

Braatne, J. H., Rood, S. B., & Heilman, P. E. (1996). Life history, ecology, and conservation of riparian cottonwoods in North America. In *Biology of populus and its implications for management and conservation, (Part I)* (pp. 57–85).

Bradford, K. J., Sharkey, T. D., & Farquhar, G. D. (1983). Gas exchange, stomatal behavior, and $\delta^{13}C$ values of the flacca tomato mutant in relation to abscisic acid. *Plant Physiology*, *72*(1), 245–250. https://doi.org/10.1104/pp.72.1.245

Brownlie, W. R., & Taylor, B. D. (1981). *Coastal sediment delivery by major rivers in Southern California (No. 17–c; Sediment management for southern California Mountains, Coastal Plains and Shoreline)*. Environmental Quality Laboratory, California Institute of Technology.
Busch, D. E., Ingraham, N. L., & Smith, S. D. (1992). Water uptake in woody riparian phreatophytes of the southwestern United States: A stable isotope study. *Ecological Applications*, *2*(4), 450–459. https://doi.org/10.2307/1941880
California Department of Water Resources (CDWR) SGMA data viewer. (2020). Sustainable groundwater management program. Retrieved from https://sgma.water.ca.gov/webgis/?appid=SGMADataViewer
Camporeale, C., Perona, P., & Ridolfi, L. (2019). Hydrological and geomorphological significance of riparian vegetation in drylands. In *Dryland ecohydrology* (pp. 239–275).
Cayan, D. R., Redmond, K. T., & Riddle, L. G. (1999). ENSO and hydrologic extremes in the Western United States. *Journal of Climate*, *12*(9), 2881–2893. https://doi.org/10.1175/1520-0442(1999)012<2881:EAHEIT>2.0.CO;2
Cernusak, L. A., Ubierna, N., Winter, K., Holtum, J. A. M., Marshall, J. D., & Farquhar, G. D. (2013). Environmental and physiological determinants of carbon isotope discrimination in terrestrial plants. *New Phytologist*, *200*(4), 950–965. https://doi.org/10.1111/nph.12423
Cooke, J. E., & Rood, S. B. (2007). Trees of the people: The growing science of poplars in Canada and worldwide. *Botany*, *85*(12), 1103–1110. https://doi.org/10.1139/B07-125
Dai, A. (2011). Characteristics and trends in various forms of the palmer drought severity index during 1900–2008. *Journal of Geophysical Research*, *116*(D12), D12115. https://doi.org/10.1029/2010JD015541
Dai, A., Trenberth, K. E., & Qian, T. (2004). A global dataset of palmer drought severity index for 1870–2002: Relationship with soil moisture and effects of surface warming. *Journal of Hydrometeorology*, *5*(6), 1117–1130. https://doi.org/10.1175/JHM-386.1
Daly, C., Halbleib, M., Smith, J. I., Gibson, W. P., Doggett, M. K., Taylor, G. H., & Pasteris, P. P. (2008). Physiographically sensitive mapping of climatological temperature and precipitation across the conterminous United States. *International Journal of Climatology*, *28*(15), 2031–2064. https://doi.org/10.1002/joc.1688
Dawson, T. E., & Ehleringer, J. R. (1998). Plants, isotopes and water use: A catchment-scale perspective. In *Isotope tracers in catchment hydrology*. Elsevier B.V. https://doi.org/10.1016/b978-0-444-81546-0.50013-6
Dawson, T. E., & Pate, J. S. (1996). Seasonal water uptake and movement in root systems of Australian phraeatophytic plants of dimorphic root morphology: A stable isotope investigation. *Oecologia*, *107*(1), 13–20. https://doi.org/10.1007/bf00582230
Downs, P. W., Dusterhoff, S. R., & Sears, W. A. (2013). Reach-scale channel sensitivity to multiple human activities and natural events: Lower Santa Clara River, California, USA. *Geomorphology*, *189*, 121–134. https://doi.org/10.1016/J.GEOMORPH.2013.01.023
Dragoni, W., & Sukhija, B. S. (2008). Climate change and groundwater: A short review. *Geological Society, London, Special Publications*, *288*(1), 1–12. https://doi.org/10.1016/j.jhydrol.2018.04.059
Drake, P. L., De Boer, H. J., Schymanski, S. J., & Veneklaas, E. J. (2019). Two sides to every leaf: Water and CO 2 transport in hypostomatous and amphistomatous leaves. *New Phytologist*, *222*(3), 1179–1187. https://doi.org/10.1111/nph.15652
Dutton, A., Wilkinson, B. H., Welker, J. M., Bowen, G. J., & Lohmann, K. C. (2005). Spatial distribution and seasonal variation in $^{18}O/^{16}O$ of modern precipitation and river water across the conterminous USA. *Hydrological Processes: International Journal*, *19*(20), 4121–4146. https://doi.org/10.1002/hyp.5876
Eggemeyer, K. D., Awada, T., Harvey, F. E., Wedin, D. A., Zhou, X., & Zanner, C. W. (2008). Seasonal changes in depth of water uptake for encroaching trees Juniperus virginiana and Pinus ponderosa and two dominant C4 grasses in a semiarid grassland. *Tree Physiology*, *29*(2), 157–169. https://doi.org/10.1093/treephys/tpn019
Ehleringer, J. R., & Dawson, T. E. (1992). Water uptake by plants: Perspectives from stable isotope composition. *Plant, Cell and Environment*, *15*(9), 1073–1082. https://doi.org/10.1111/j.1365-3040.1992.tb01657.x
Evans, R. D., & Ehleringer, J. R. (1994). Water and nitrogen dynamics in an arid woodland. *Oecologia*, *99*(3–4), 233–242. https://doi.org/10.1007/BF00627735
Farooq, M., Hussain, M., Wahid, A., Siddique, K. H. M., & Aroca, R. (2012). Drought stress in plants: An overview. In *Plant responses to drought stress: From morphological to molecular features* (pp. 1–33). Springer Berlin Heidelberg. https://doi.org/10.1007/978-3-642-32653-0
Farquhar, G. D., Ehleringer, L. R., & Hubic, K. T. (1989). Carbon isotope discrimination and photosynthesis. *Annual Review of Plant Physiology and Plant Molecular Biology*, *40*(1), 503–537. https://doi.org/10.1146/annurev.arplant.40.1.503
Ferris, R., Long, L., Bunn, S. M., Robinson, K. M., Bradshaw, H. D., Rae, A. M., & Taylor, G. (2002). Leaf stomatal and epidermal cell development: Identification of putative quantitative trait loci in relation to elevated carbon dioxide concentration in poplar. *Tree Physiology*, *22*(9), 633–640. https://doi.org/10.1093/treephys/22.9.633
Fichot, R., Brignolas, F., Cochard, H., & Ceulemans, R. (2015). Vulnerability to drought-induced cavitation in poplars: Synthesis and future opportunities. *Plant, Cell and Environment*, *38*(7), 1233–1251. https://doi.org/10.1111/pce.12491
Flanagan, L. B., Orchard, T. E., Tremel, T. N., & Rood, S. B. (2019). Using stable isotopes to quantify water sources for trees and shrubs in a riparian cottonwood ecosystem in flood and drought years. *Hydrological Processes*, *33*(24), 3070–3083. https://doi.org/10.1002/hyp.13560
Francey, R. J., & Farquhar, G. D. (1982). An explanation of 13C/12C variations in tree rings. *Nature*, *297*(5861), 28–31. https://doi.org/10.1038/297028a0
Gebauer, R. L. E., & Ehleringer, J. R. (2000). Water and nitrogen uptake patterns following moisture pulses in a cold desert community. *Ecology*, *81*(5), 1415–1424. https://doi.org/10.1890/0012-9658(2000)081[1415:WANUPF]2.0.CO;2
Gessler, A., Cailleret, M., Joseph, J., Schönbeck, L., Schaub, M., Lehmann, M., et al. (2018). Drought induced tree mortality – A tree-ring isotope based conceptual model to assess mechanisms and predispositions. *New Phytologist*, *219*(2), 485–490. https://doi.org/10.1111/nph.15154
Gessler, A., Ferrio, J. P., Hommel, R., Treydte, K., Werner, R. A., & Monson, R. K. (2014). Stable isotopes in tree rings: Towards a mechanistic understanding of isotope fractionation and mixing processes from the leaves to the wood. *Tree Physiology*, *34*(8), 796–818. https://doi.org/10.1093/treephys/tpu040
Ghazavi, R., & Ebrahimi, H. (2018). Predicting the impacts of climate change on groundwater recharge in an arid environment using modeling approach. *International Journal of Climate Change Strategies and Management*, *11*(1), 88–99. https://doi.org/10.1108/ijccsm-04-2017-0085
Gorelick, N., Hancher, M., Dixon, M., Ilyushchenko, S., Thau, D., & Moore, R. (2017). Google Earth Engine: Planetary-scale geospatial analysis for everyone. *Remote Sensing of Environment*, *202*, 18–27. https://doi.org/10.1016/j.rse.2017.06.031
Gornall, J. L., & Guy, R. D. (2007). Geographic variation in ecophysiological traits of black cottonwood (Populus trichocarpa). *Botany*, *85*(12), 1202–1213. https://doi.org/10.1139/B07-079
Guo, J. S., Bush, S. E., & Hultine, K. R. (2022). Temporal variation in stomatal sensitivity to vapour pressure deficit in western riparian forests. *Functional Ecology*, *36*(7), 1599–1611. https://doi.org/10.1111/1365-2435.14066
Hall, L. S., Orr, B. K., Hatten, J., Lambert, A., & Dudley, T. L. (2020). Final report: Southwestern Willow Flycatcher (Empidonax traillii extimus) and Western yellow-billed cuckoo (Coccyzus americanus occidentalis) surveys and habitat availability modeling on the Santa Clara River,

California, 26 March 2020. In *[Other government series]*. Western Foundation of Vertebrate Zoology - Field Projects. Retrieved from http://pubs.er.usgs.gov/publication/70217199

Hanson, R. T., Flint, L. E., Flint, A. L., Dettinger, M. D., Faunt, C. C., Cayan, D., & Schmid, W. (2012). A method for physically based model analysis of conjunctive use in response to potential climate changes. *Water Resources Research*, *48*(6), W00L08. https://doi.org/10.1029/2011WR010774

Howe, W. H., & Knopf, F. L. (1991). On the imminent decline of Rio Grande cottonwoods in Central New Mexico. *Southwestern Naturalist*, *36*(2), 218–224. https://doi.org/10.2307/3671924

Hultine, K. R., Bush, S. E., & Ehleringer, J. R. (2010). Ecophysiology of riparian cottonwood and willow before, during, and after two years of soil water removal. *Ecological Applications*, *20*(2), 347–361. https://doi.org/10.1890/09-0492.1

Hultine, K. R., Froend, R., Blasini, D., Bush, S. E., Karlinski, M., & Koepke, D. F. (2020). Hydraulic traits that buffer deep-rooted plants from changes in hydrology and climate. *Hydrological Processes*, *34*(2), 209–222. https://doi.org/10.1002/hyp.13587

Keeling, C. D., Stephen, C., Piper, S. C., Bacastow, R. B., Wahlen, M., Whorf, T. P., et al. (2001). *Exchanges of atmospheric CO_2 and $^{13}CO_2$ with the terrestrial biosphere and oceans from 1978 to 2000* (pp. 1–28). Scripps Institution of Oceanography. Retrieved from https://escholarship.org/uc/item/09v319r9

Kibler, C. L., Schmidt, E. C., Roberts, D. A., Stella, J. C., Kui, L., Lambert, A. M., & Singer, M. B. (2021). A brown wave of riparian woodland mortality following groundwater declines during the 2012-2019 California drought. *Environmental Research Letters*, *16*(084030), 1–12. https://doi.org/10.1088/1748-9326/ac1377

Kibler, C. L., Trugman, A. T., Roberts, D. A., Still, C. J., Scott, R. L., Caylor, K. K., et al. (2023). Evapotranspiration regulates leaf temperature and respiration in dryland vegetation. *Agricultural and Forest Meteorology*, *339*, 109560. https://doi.org/10.1016/j.agrformet.2023.109560

Klein, T., Shpringer, I., Fikler, B., Elbaz, G., Cohen, S., & Yakir, D. (2013). Relationships between stomatal regulation, water-use, and water-use efficiency of two coexisting key Mediterranean tree species. *Forest Ecology and Management*, *302*, 34–42. https://doi.org/10.1016/j.foreco.2013.03.044

Krueper, D. J. (1993). Effects of land use practices on western riparian ecosystems. *Status and Management of Neotropical Migratory Birds*, 321–330.

Kui, L., & Kibler, C. (2023). Oxygen isotope in plants and source water between 2018 and 2020, along the Santa Clara River, CA ver 1 [Dataset]. *Environmental Data Initiative*. https://doi.org/10.6073/pasta/98b1154256c7f7547c6a0e2b6e191560

Leffler, A. J., England, L. E., & Naito, J. (2000). Vulnerability of Fremont cottonwood (Populus fremontii Wats.) individuals to xylem cavitation. *Western North American Naturalist*, 204–210.

Li, H., Li, Z., Chen, Y., Xiang, Y., Liu, Y., Kayumba, P. M., & Li, X. (2021). Drylands face potential threat of robust drought in the CMIP6 SSPs scenarios. *Environmental Research Letters*, *16*(11), 114004. https://doi.org/10.1088/1748-9326/ac2bce

Lipiec, J., Doussan, C., Nosalewicz, A., & Kondracka, K. (2013). Effect of drought and heat stresses on plant growth and yield: A review. *International Agrophysics*, *27*(4), 463–477. https://doi.org/10.2478/intag-2013-0017

Lite, S. J., & Stromberg, J. C. (2005). Surface water and ground-water thresholds for maintaining Populus-Salix forests, San Pedro River, Arizona. *Biological Conservation*, *125*(2), 153–167. https://doi.org/10.1016/j.biocon.2005.01.020

Luo, L., Apps, D., Arcand, S., Xu, H., Pan, M., & Hoerling, M. (2017). Contribution of temperature and precipitation anomalies to the California drought during 2012–2015. *Geophysical Research Letters*, *44*(7), 3184–3192. https://doi.org/10.1002/2016GL072027

Mann, M. E., & Gleick, P. H. (2015). Climate change and California drought in the 21st century. *Proceedings of the National Academy of Sciences of the United States of America*, *112*(13), 3858–3859. https://doi.org/10.1073/pnas.1503667112

Martin-StPaul, N., Delzon, S., & Cochard, H. (2017). Plant resistance to drought depends on timely stomatal closure. *Ecology Letters*, *20*(11), 1437–1447. https://doi.org/10.1111/ele.12851

Mayes, M., Caylor, K. K., Singer, M. B., Stella, J. C., Roberts, D., & Nagler, P. (2020). Climate sensitivity of water use by riparian woodlands at landscape scales. *Hydrological Processes*, *34*(25), 4884–4903. https://doi.org/10.1002/hyp.13942

McCarroll, D., & Loader, N. J. (2004). Stable isotopes in tree rings. *Quaternary Science Reviews*, *23*(7–8), 771–801. https://doi.org/10.1016/j.quascirev.2003.06.017

Moreno-Gutiérrez, C., Battipaglia, G., Cherubini, P., Saurer, M., Nicolás, E., Contreras, S., & Querejeta, J. I. (2012). Stand structure modulates the long-term vulnerability of Pinus halepensis to climatic drought in a semiarid Mediterranean ecosystem. *Plant, Cell and Environment*, *35*(6), 1026–1039. https://doi.org/10.1111/j.1365-3040.2011.02469.x

National Resource Council (NRC). (2002). *Riparian areas: Functions and strategies for management*. The National Academies Press. https://doi.org/10.17226/10327

Orr, B. K., Diggory, Z. E., Coffman, G. C., Sears, W. I. A., Dudley, T. L., & Merrill, A. G. (2011). Riparian vegetation classification and mapping: Important tools for large-scale river corridor restoration in a semi-arid landscape (pp. 212–232).

Palmer, W. C. (1965). *Meteorological drought* (Vol. 30). US Department of Commerce.

Patten, D. T. (1998). Riparian ecosystems of semi-arid North America: Diversity and human impacts. *Wetlands*, *18*(4), 498–512. https://doi.org/10.1007/bf03161668

Phelan, C. A., Pearce, D. W., Franks, C. G., Zimmerman, O., Tyree, M. T., & Rood, S. B. (2022). How trees thrive in a dry climate: Diurnal and seasonal hydrology and water relations in a riparian cottonwood grove. *Tree Physiology*, *42*(1), 99–113. https://doi.org/10.1093/treephys/tpab087

Pirasteh-Anosheh, H., Saed-Moucheshi, A., Pakniyat, H., & Pessarakli, M. (2016). Stomatal responses to drought stress. Water stress and crop plants: A sustainable approach. *Geophysical Research Letters*, *1*, 24–40. https://doi.org/10.1002/9781119054450.ch3

Pockman, W. T., & Sperry, J. S. (2000). Vulnerability to xylem cavitation and the distribution of Sonoran desert vegetation. *American Journal of Botany*, *87*(9), 1287–1299. https://doi.org/10.2307/2656722

Ponton, S., Dupouey, J. L., Bréda, N., Feuillat, F., Bodenes, C., & Dreyer, E. (2001). Carbon isotope discrimination and wood anatomy variations in mixed stands of Quercus robur and Quercus petraea. *Plant, Cell and Environment*, *24*(8), 861–868. https://doi.org/10.1046/j.0016-8025.2001.00733.x

R Core Team. (2022). *R: A language and environment for statistical computing*. R Foundation for Statistical Computing. Retrieved from https://www.R-project.org/

Robeson, S. M. (2015). Revisiting the recent California drought as an extreme value. *Geophysical Research Letters*, *42*(16), 6771–6779. https://doi.org/10.1002/2015GL064593

Roden, J. S., Lin, G., & Ehleringer, J. R. (2000). A mechanistic model for interpretation of hydrogen and oxygen isotope ratios in tree-ring cellulose-Evidence and implications for the use of isotopic signals transduced by plants. *Geochimica et Cosmochimica Acta*, *64*(1), 21–35. https://doi.org/10.1016/S0016-7037(99)00195-7

Rood, S. B., Ball, D. J., Gill, K. M., Kaluthota, S., Letts, M. G., & Pearce, D. W. (2013). Hydrologic linkages between a climate oscillation, river flows, growth, and wood $\Delta^{13}C$ of male and female cottonwood trees. *Plant, Cell and Environment*, *36*(5), 984–993. https://doi.org/10.1111/pce.12031

Rood, S. B., Bigelow, S. G., & Hall, A. A. (2011). Root architecture of riparian trees: River cut-banks provide natural hydraulic excavation, revealing that cottonwoods are facultative phreatophytes. *Trees - Structure and Function*, *25*(5), 907–917. https://doi.org/10.1007/s00468-011-0565-7

Rood, S. B., Braatne, J. H., & Hughes, F. M. R. (2003). Ecophysiology of riparian cottonwoods: Stream flow dependency, water relations and restoration. *Tree Physiology*, *23*(16), 1113–1124. https://doi.org/10.1093/treephys/23.16.1113

Rood, S. B., Patiño, S., Coombs, K., & Tyree, M. T. (2000). Branch sacrifice: Cavitation-associated drought adaptation of riparian cottonwoods. *Trees*, *14*(5), 248–257. https://doi.org/10.1007/s004680050010

Sabathier, R., Singer, M. B., Stella, J. C., Roberts, D. A., & Caylor, K. K. (2021). Vegetation responses to climatic and geologic controls on water availability in southeastern Arizona. *Environmental Research Letters*, *16*(6), 064029. https://doi.org/10.1088/1748-9326/abfe8c

Sargeant, C. I., & Singer, M. B. (2016). Sub-annual variability in historical water source use by Mediterranean riparian trees. *Ecohydrology*, *9*(7), 1328–1345. https://doi.org/10.1002/eco.1730

Sargeant, C. I., Singer, M. B., & Vallet-Coulomb, C. (2019). Identification of source - Water oxygen isotopes in trees toolkit (ISO - Tool) for deciphering historical water use by forest trees water resources research. *Water Resources Research*, 1–22. https://doi.org/10.1029/2018WR024519

Sarris, D., Siegwolf, R., & Körner, C. (2013). Inter- and intra-annual stable carbon and oxygen isotope signals in response to drought in Mediterranean pines. *Agricultural and Forest Meteorology*, *168*, 59–68. https://doi.org/10.1016/j.agrformet.2012.08.007

Scheidegger, Y., Saurer, M., Bahn, M., & Siegwolf, R. (2000). Linking stable oxygen and carbon isotopes with stomatal conductance and photosynthetic capacity: A conceptual model. *Oecologia*, *125*(3), 350–357. https://doi.org/10.1007/s004420000466

Schulte, P. J., Hinckley, T. M., & Stettler, R. F. (1987). Stomatal responses of Populus to leaf water potential. *Canadian Journal of Botany*, *65*(2), 255–260. https://doi.org/10.1139/b87-036

Scott, M. L., Shafroth, P. B., & Auble, G. T. (1999). Responses of riparian cottonwoods to alluvial water table declines. *Environmental Management*, *23*(3), 347–358. https://doi.org/10.1007/s002679900191

Siegwolf, R. T., Lehmann, M. M., Goldsmith, G. R., Churakova, O. V., Mirande-Ney, C., Timoveeva, G., et al. (2023). Updating the dual C and O isotope—Gas-exchange model: A concept to understand plant responses to the environment and its implications for tree rings. *Plant, Cell and Environment*, *46*(9), 2606–2627. https://doi.org/10.1111/pce.14630

Singer, M. B., Sargeant, C. I., Piégay, H., Riquier, J., Wilson, R. J., & Evans, C. M. (2014). Floodplain ecohydrology: Climatic, anthropogenic, and local physical controls on partitioning of water sources to riparian trees. *Water Resources Research*, *50*(5), 4490–4513. https://doi.org/10.1002/2014WR015581

Singer, M. B., Stella, J. C., Dufour, S., Piégay, H., Wilson, R. J. S., & Johnstone, L. (2013). Contrasting water-uptake and growth responses to drought in co-occurring riparian tree species. *Ecohydrology*, *6*(3), 402–412. https://doi.org/10.1002/eco.1283

Snyder, K. A., & Williams, D. G. (2000). Water sources used by riparian trees varies among stream types on the San Pedro River, Arizona. *Agricultural and Forest Meteorology*, *105*(1–3), 227–240. https://doi.org/10.1016/S0168-1923(00)00193-3

Sparks, J. P., & Ehleringer, J. R. (1997). Leaf carbon isotope discrimination and nitrogen content for riparian trees along elevational transects. *Oecologia*, *109*(3), 362–367. https://doi.org/10.1007/s004420050094

Stella, J. C., & Bendix, J. (2019). Multiple stressors in riparian ecosystems. In *Multiple stressors in river ecosystems: Status, impacts and prospects for the future* (pp. 81–110). Elsevier Inc. https://doi.org/10.1016/B978-0-12-811713-2.00005-4

Stella, J. C., Rodriguez-Gonzalez, P. M., Dufour, S., & Bendix, J. (2013). Riparian vegetation research in Mediterranean-climate regions: Common patterns, ecological processes, and considerations for management. *Mediterranean Climate Streams*, *719*(1), 291–315. https://doi.org/10.1007/s10750-012-1304-9

Stillwater Sciences. (2019). *Vegetation mapping of the Santa Clara River, Ventura county and Los Angeles County, California*. Technical Memorandum. Prepared by Stillwater Sciences, Berkeley, California for the Western Foundation of Vertebrate Zoology.

Stolar, R. (2019). *Populus fremontii tree ring analysis and semi-arid river water source variability over time, San Pedro River, Arizona*. Doctoral dissertation, The University of Arizona.

Stromberg, J. C. (1993). Fremont cottonwood-Goodding willow riparian forests: A review of their ecology, threats, and recovery potential. *Journal of the Arizona-Nevada Academy of Science*, 97–110.

Stromberg, J. C., Tiller, R., & Richter, B. (1996). Effects of groundwater decline on riparian vegetation of semiarid regions: The San Pedro, Arizona. *Ecological Society of America*, *6*(1), 113–131. https://doi.org/10.2307/2269558

Teskey, R., Wertin, T., Bauweraerts, I., Ameye, M., McGuire, M. A., & Steppe, K. (2015). Responses of tree species to heat waves and extreme heat events. *Plant, Cell and Environment*, *38*(9), 1699–1712. https://doi.org/10.1111/pce.12417

Treydte, K., Boda, S., Graf Pannatier, E., Fonti, P., Frank, D., Ullrich, B., et al. (2014). Seasonal transfer of oxygen isotopes from precipitation and soil to the tree ring: Source water versus needle water enrichment. *New Phytologist*, *202*(3), 772–783. https://doi.org/10.1111/nph.12741

U.S. Drought Monitor. (2021). Time series for the Santa Clara River watershed. Retrieved from https://droughtmonitor.unl.edu

Voltas, J., Lucabaugh, D., Chambel, M. R., & Ferrio, J. P. (2015). Intraspecific variation in the use of water sources by the circum-Mediterranean conifer Pinus halepensis. *New Phytologist*, *208*(4), 1031–1041. https://doi.org/10.1111/nph.13569

Wang, H., Rogers, J. C., & Munroe, D. K. (2015). Commonly used drought indices as indicators of soil moisture in China. *Journal of Hydrometeorology*, *16*(3), 1397–1408. https://doi.org/10.1175/JHM-D-14-0076.1

Wang, T., Wu, Z., Wang, P., Wu, T., Zhang, Y., Yin, J., et al. (2023). Plant-groundwater interactions in drylands: A review of current research and future perspectives. *Agricultural and Forest Meteorology*, *341*, 109636. https://doi.org/10.1016/j.agrformet.2023.109636

Warter, M. M., Singer, M. B., Cuthbert, M. O., Roberts, D., Caylor, K. K., Sabathier, R., & Stella, J. (2021). Drought onset and propagation into soil moisture and grassland vegetation responses during the 2012-2019 major drought in Southern California. *Hydrology and Earth System Sciences*, *25*(6), 3713–3729. https://doi.org/10.5194/hess-25-3713-2021

Wells, N., Goddard, S., & Hayes, M. J. (2004). A self-calibrating palmer drought severity index. *Journal of Climate*, *17*(12), 2335–2351. https://doi.org/10.1175/1520-0442(2004)017<2335:aspdsi>2.0.co;2

Williams, J. (2022). Tree-ring width measurements and isotope data for riparian Populus species, Santa Clara River, 2019 ver 2 [Dataset]. *Environmental Data Initiative*. https://doi.org/10.6073/pasta/7122c4d4a72954bc1ddef74f03560879

Williams, J., Stella, J. C., Voelker, S. L., Lambert, A. M., Pelletier, L. M., Drake, J. E., et al. (2022). Local groundwater decline exacerbates response of dryland riparian woodlands to climatic drought. *Global Change Biology*, *28*(22), 6771–6788. https://doi.org/10.1111/gcb.16376

Zimmerman, O. R., Pearce, D. W., Woodman, S. G., Rood, S. B., & Flanagan, L. B. (2023). Increasing contribution of alluvial groundwater to riparian cottonwood forest water use through warm and dry summers. *Agricultural and Forest Meteorology*, *329*, 109292. https://doi.org/10.1016/j.agrformet.2022.109292

References From the Supporting Information

Bowen, G. J. (2017). The online isotopes in precipitation calculator, version 3.1. Retrieved from http://www.waterisotopes.org

Bowen, G. J., Wassenaar, L. I., & Hobson, K. A. (2005). Global application of stable hydrogen and oxygen isotopes to wildlife forensics. *Oecologia*, *143*(3), 337–348. https://doi.org/10.1007/s00442-004-1813-y

Copenheaver, C. A., Gärtner, H., Schäfer, I., Vaccari, F. P., & Cherubini, P. (2010). Drought-triggered false ring formation in a Mediterranean shrub. *Botany*, *88*(6), 545–555. https://doi.org/10.1139/B10-029

Farid, A., Goodrich, D. C., Bryant, R., & Sorooshian, S. (2008). Using airborne lidar to predict Leaf Area Index in cottonwood trees and refine riparian water-use estimates. *Journal of Arid Environments*, *72*(1), 1–15. https://doi.org/10.1016/j.jaridenv.2007.04.010

Hoffer, M., & Tardif, J. C. (2009). False rings in jack pine and black spruce trees from eastern Manitoba as indicators of dry summers. *Canadian Journal of Forest Research*, *39*(9), 1722–1736. https://doi.org/10.1139/X09-088

Horton, J. L., Kolb, T. E., & Hart, S. C. (2001). Responses of riparian trees to interannual variation in ground water depth in a semi-arid river basin. *Plant, Cell and Environment*, *24*(3), 293–304. https://doi.org/10.1046/j.1365-3040.2001.00681.x

Kui, L., & Kibler, C. (2023). Oxygen isotope in plants and source water between 2018 and 2020, along the Santa Clara River, CA Ver 1 [Dataset]. *Environmental Data Initiative*. https://doi.org/10.6073/PASTA/98B1154256C7F7547C6A0E2B6E191560

Majoube, M. (1971). Oxygen-18 and deuterium fractionation between water and steam. *Journal de Chimie Physique et de Physico-Chimie Biologique*, *68*, 1423–1436. https://doi.org/10.1051/jcp/1971681423

Pataki, D. E., Bush, S. E., Gardner, P., Solomon, D. K., & Ehleringer, J. R. (2005). Ecohydrology in a Colorado River riparian forest: Implications for the decline of Populus fremontii. *Ecological Applications*, *15*(3), 1009–1018. https://doi.org/10.1890/04-1272

Schomaker, M. (2007). *Crown-condition classification: A guide to data collection and analysis (No. 102)*. US Department of Agriculture, Forest Service.